New results and questions of lunar exploration from SELENE, Chang'E-1, Chandrayaan-1 and LRO/LCROSS

Shuanggen Jin [a,*], Sundaram Arivazhagan [b,c], Hiroshi Araki [d]

[a] *Shanghai Astronomical Observatory, Chinese Academy of Sciences, Shanghai 200030, China*
[b] *PLANEX, Physical Research Laboratory, Ahmedabad 380 009, India*
[c] *CGIPS, Department of Geology, Periyar University, Salem 636 011, India*
[d] *National Astronomical Observatory of Japan, Tokyo 181-8588, Japan*

Available online 1 December 2012

Abstract

The moon has longstanding questions such as lunar environments, origin, formation and evolution, magnetization of crustal rocks, internal structure and possible life. The recent lunar missions, e.g., SELenological and ENgineering Explorer "KAGUYA" (SELENE), Chang'E-1, Chandrayaan-1, and Lunar Reconnaissance Orbiter/Lunar CRater Observation and Sensing Satellite (LRO/LCROSS), have provided new opportunities to explore and understand these issues. In this paper, we reviewed and presented the results and findings in the fields of lunar gravity, magnetic field, atmosphere, surface geomorphology and compositional variations, volcano, craters, internal structure, water and life science from new lunar exploration missions. In addition, the new objectives and scientific questions on lunar explorations in near future are presented and discussed.
© 2012 COSPAR. Published by Elsevier Ltd. All rights reserved.

Keywords: Lunar exploration; SELENE; Chang'E-1; Chandrayaan-1; LRO/LCROSS

1. Introduction

The moon is our nearest celestial neighbor, and because of its proximity, it is considered as a probable base station for space programs in near future due to the reduction of cost and time. As water is the primary source of life, the first search on moon was initiated with the search of water traces. The presence of water in good amount is more advantageous because, water can be utilized as fuel source for rockets and it makes possibility of the human settlement on the moon. Furthermore, the moon is also viewed as a possible future source of economic minerals (Stephen and Gillett, 1992). The studies showed that the moon has practically no atmosphere and lost its thermal energy in the initial stages of formation, so it has undergone meager change from its earlier formation unlike the Earth, which has undergone drastic changes.

The anhydrous nature of the lunar materials precludes any formation of ore deposits like Earth. The moon is more heterogeneous and it underwent prolonged igneous activity with spanning hundreds of millions of years. This process led to varied and large-scale differentiation and fractionation during its early history. The mere waterlessness of the lunar environment does not preclude the all ore-forming process. The ore deposits can be formed through magmatic process of partial melting, fractional crystallization and phase separation. Examples of such magmatic deposits ores on the Earth include Cu–Ni sulfide ores from sulfide immiscibility, chromite from cumulate settling and magnetite ores crystallized from late-stage magmatic fluids. Similar process can occur on the moon too (Warren and Bridges, 2004). Therefore, there are a number of unknown and longstanding questions on the moon, such as lunar environments, origin, formation and evolution, magnetization of crustal rocks, internal structure and possible life (Jin, 2012). Furthermore, the moon rocks can provide the crucial insight into the early development of the earth and other planets (Warren and Bridges, 2004).

---

* Corresponding author. Tel.: +86 21 34775292; fax: +86 21 64384618.
  E-mail addresses: sgjin@shao.ac.cn, sg.jin@yahoo.com (S. Jin).

In 1960, US made its first attempt to obtain closer images of lunar surface with Ranger series. Since then, lunar exploration has gained a phenomenal interest all over the world. These explorations provided new understanding and insights on moon. Lunar mare basalts, highland anorthosites and KREEP (K – potassium, REE – Rare Earth Elements) and P (-phosphorus) are the three major lunar rock types reported from the lunar surface and relative to the Earth, so the moon has a strong depletion of volatile elements, water and a probable enrichment of refractory elements. The recent results from various missions are challenging our previous understanding including identification of ice on Polar Regions, OH/H_2O, and new mineral identification like Spinel. Despite of the fact that Apollo and later lunar missions had greatly helped our understanding of the moon, however many gaps are still left out. In this circumstance, number of questions like the lunar evolution, age, off- center of gravity, the unequal distribution of the lunar crust material in near and far sides, the complexity of crater, and presence of olivine in the center of some large craters are yet to be explained. Also, the origin, evolution and deep interior of the moon as well as surface processes and possible life on moon remain mysterious. One of the main factors for this lack of understanding is that the whole surface of the moon has not yet been imagined/sampled in a homogeneous manner. Several countries have shown interests in exploring the moon in recent years. The current lunar missions have provided new opportunities to explore and understand the moon in more details with higher spatial and spectral resolution. In this manuscript, we have reviewed and presented the new results and findings from recent lunar exploration missions and scientific questions on the moon are discussed with the future lunar missions.

2. The recent lunar missions and exploration

Lunar geologic mapping started in the late 1960s when five Lunar Orbiter (LO) missions launched in 1966 and 1967, providing an excellent photographic image at ~99% coverage (Hansen, 1970). Exploration of lunar geology was intensified after the successful landing of the Apollo 11 mission in 1969. Since then, it has been carried out to understand the chemistry, mineralogy and rock types of the moon. The moon has not been geologically mapped in a systematic fashion for more than 25 years, and some major advances in lunar science have occurred in the last 15 years.

The Apollo lunar missions have returned with a wealth of data in the form of lunar rocks and minerals, ground truth measurements, orbital remote sensing, and field mapping by astronauts which helped to characterize the geology of six locations in great details. The sample return missions and Soviet robotic rovers have contributed substantially to understand the moon (Robinson and Riner, 2005). Both Apollo and Lunar missions carried around 380 kg of rock and soil samples to Earth with a limitation

of small number of nearside equatorial regions on the moon. For the first time, Clementine and Lunar Prospector missions have provided a global view of the remote sensing data to study the lunar surface composition, complete view of the shape, gravity and magnetic anomalies associated with moon (Dunkin and Heather, 2000). Earth-based telescopic observations (1990) and Galileo lunar flybys (1992) have proven the scientific potential of digital multispectral imaging to develop our perceptive of the moon. The Clementine spacecraft orbited the moon for 10 weeks in 1994 and transmitted around 35 GB of scientific data and through that significant progress have been made by lunar science community (Nozette et al., 1994; McEwen and Robinson, 1997). Direct link observed in between the high resolution (100–500 m) visible to near-infrared (VNIR) remote sensing data and laboratory spectral data and geochemical/ mineralogical analyses of Apollo and Luna samples (McCallum, 2001). Lunar surface abundance maps were prepared by using Lunar Prospector (LP) measured gamma rays and neutrons in 1998–1999 from the lunar surface at a scale of 30–150 km/pixel (Binder, 1998).

Beyond that, several countries have recently explored the lunar surface for source of economic minerals and to understand the early development of the moon, Earth and other planets. The important recent lunar exploration missions are Japan's Kaguya (SELENE) that was launched on 14th September 2007 to obtain scientific data of the lunar origin and evolution and to develop the technology for the future lunar exploration, China's Chang'E-1 Lunar Orbiter launched on 24th October 2007 to study the lunar environment and 3-D surface topography. India's orbital satellite Chandrayaan-1 launched on 22nd October 2008 and USA's Lunar Reconnaissance Orbiter/Lunar CRater Observation and Sensing Satellite (LRO/LCROSS) launched on 18th June 2009 to search for water ice in a permanently shadowed crater near one of the moon's poles. In addition, on 10th September 2011, the NASA's Discovery Program Gravity Recovery and Interior Laboratory (GRAIL) was launched to get high-quality gravitational field mapping of the moon to determine its interior structure. Their main instruments and payloads are shown in Table 1.

3. New results from recent lunar missions

3.1. New findings of SELENE

SELENE is a Japanese lunar exploration mission, launched to obtain scientific data for the study of origin and evolution of the moon. The Multi Imager (MI) sensor found the 1250 nm plagioclase absorption band in the lunar surface (Ohtake et al., 2009). The historical lunar orbiters observations had limitation in terms of spectral and spatial resolution and restricted the detailed information on the lunar surface mineral composition. Spectral Profiler (SP) performed global spectroscopic mapping of the moon with unprecedented accuracy, broad spectral

Table 1
Scientific instrument for Chang'E-1, SELENE, Chandrayaan-1 and LRO/LCROSS missions.

Instruments	Chang'E-1 (China, 2007)	Specification	SELENE (Japan, 2007)	Specification	Chandrayaan-1 (India, 2008)	Specification	LRO (USA, 2009)	Specification
Stereo imager	X	Spectral range: 0.5–0.75 μm Spatial resolution: 120 m/pixel Swath: 60 km	X	Spectral range: 0.43–0.85 μm Spatial resolution: 10 m/pixel Swath:40 km	X	Spectral range: 0.5–0.75 μm Spatial resolution: 5 m/pixel Swath: 20 km	X	NAC Spectral range: 0.55 μm Spatial resolution: 0.5 m/pixel Swath: 5 km WAC Spectral range: 0.3–0.68 μm Spatial resolution: 100 m/pixel Swath: 5 km
VNIR camera	X	Spectral range: 0.48–0.96 μm Spatial resolution: 200 m/pixel Swath: 25.6 km. No. of channels: 32	X	VIS: 0.415 ; 0.75;0.9; 0.95; 1.0 μm Spatial resolution:20 m Swath: 20 km NIR: 1.0; 1.05; 1.25; 1.55 μm Spatial resolution: 62 m Swath:20 km No. of channels: 9	X	Spectral range: 0.4–0.9 μm Spatial resolution: 80 m/pixel Swath: 20 km No. of channels: 64-		
UV Imager	–						X	Spectral range: 57–187 nm Spatial resolution: 260 m/pixel; Swath: 5 km
IR spectrometer	–		X	Spectral range: 0.5–2.6 μm Spatial resolution : 500 m/pixel Swath:19.3 km	X	Spectral range: 0.45–3 μm & Spatial resolution: 140 m/pixel Swath : 42.5 km		
Magnetometer	–		X	Dynamic range Resolution	Range-3: ±65536 nT range-2: ± 1024 nT range-1: ±256 nT range-0: ±64 nT Range-3: 2.0 nT range-2: 0.03 nT range-1: 0.008 nT range-0: 0.002 nT			
X-ray spectrometer	X	Effective area: 17 cm^2. Energy range: 1–60 keV. Spatial resolution.170 × 170 km Altitude: 200 km. Energy range of solar monitor: 1–10 keV. Energy resolution of solar monitor: ⩽600 eV at 5.95 keV	X	Energy range: 1–10 keV, Spatial resolution: 20 km	X	Energy range: 30–270 keV Spatial resolution: 33 km		

Table 1 (*continued*)

Instruments	Chang'E-1 (China, 2007)	Specification	SELENE (Japan, 2007)	Specification	Chandrayaan-1 (India, 2008)	Specification	LRO (USA, 2009)	Specification
γ-ray experiment	X	Energy: 300–9000 keV. Number of energy bands: 512 or 1024	X	Energy: 0.1–10 MeV Spatial resolution: 100 km				
Neutron detector							X	Spectral range : 15 MeV Spatial resolution: 50 km Sensitivity : 100 ppm
Laser altimeter	X	Range of distance measurement: 200 ± 25 km. Footprint on the lunar surface: ⩽Φ200 m. Spectral range: 1064 nm. Energy: 150 mJ. Laser pulse width: 5–7 ns. Repetition rate of laser pulse: 1 Hz.	X	Energy: 100 mJ Spectral range: Spatial resolution: 1600 m	X	Energy: 10 mJ Sp. range: 1064 nm Spatial resolution: ∼5 m	X	Spectral range: 10 cm Range window: 20–70 km Spatial resolution: 5–25 m
Plasma/Ion experiments	X	Energy range: 0.05–20 keV. No. of energy bands: 48. Velocity of solar wind: 150–2000 km/s. Instantaneous field of view: 6.7° × 180° Acceptance angle: 6.7° × 15°	X	Energy range: 5–28 keV	X	Energy range: 10 eV–15 keV Mass range: 1-0 Mass resolution H+, He^{++}, He$^+$, O^{++}, O$^+$		Spectral range: spectra 0.2 keV/μm–7 MeV/μm Spatial resolution: 77 km
Sub-Kev atom reflecting analyzer					X	Energy range: 10 eV–3.2 KeV Mass range: 1–56 Mass resolution: H,O,NA/Mg/Si/Al K/Ca, Fe		
Microwave sounder	X	Frequency channels: 3.0, 7.8, 19.35, and 37 GHz. Brightness temperature sensitivity: ⩽0.5 K. Linearity: ⩽0.99. Spatial resolution: 30.50 km	X	Frequency: 4–6 MHz Spatial resolution: 75 m/pixel Swath: 5 km	X	Spectral range: 12.6 cm Frequency: 2.38 GHz; Spatial resolution 150 m pixel Swath: 10 km	X	Spectral range: 12.6 and 4.2 cm; Frequency: 2.38 GHz and 7.1 GHz Spatial resolution: 7.5–75 m/pixel Swath: 10 and 6 km
Thermal emission radiometer							X	0.3 and 400 μm (reflected – 2 bands; emitted – 7 bands) Spatial resolution: 200 m
Radiation dose monitor					X	Electons: ⩾0.85 MeV; Protons: ⩽17.5 MeV		
Penetrator/Impactor					X	600 Kg	X	2300 kg

coverage, high spectral and spatial resolution, which are necessary for the determination of lunar surface minerals. The SP identified the global distribution of the olivine concentration in the central peaks of the lunar surface (Yamamoto et al., 2010). Hawke et al. (2003) utilized Earth based telescopic spectra, Galileo image data and Clementine image data to map the distribution and occurrences of anorthosite across the entire moon and interpreted that, the upper portion of the lunar crust is composed of anorthosite layer globally and underlain by a mafic rich layer. Relatively small areas (2–10 km) of the lunar surface and numerous pure anorthosite (plagioclase > 90%) deposits were identified using combinations of VNIR telescopic spectral observations with remotely sensed multispectral data (Stoffler et al., 1980). The plagioclase absorption was identified at 1250 nm with low FeO and TiO_2 concentration (Spudis et al., 1984), e.g., Inner Rook Mountain and Orientale basin. Ohtake et al. (2009) reported the global distribution of rocks with high plagioclase abundance (∼100 vol.%) using clear plagioclase absorption band recorded by the SELENE MI, where previous estimates of 82–92 vol.% (Tompkins and Pieters, 1999; Wieczorek et al., 2006) which has provided a valuable constraint on models of lunar magma ocean (LMO) evolution.

3.1.1. Global distribution of olivine

The SP on SELENE has obtained continuous spectral reflectance data for about seventy million points on the surface of the moon over the 0.5–2.6 μm electromagnetic region with a spectral resolution of 6–8 nm acquired in the period of November 2007 to June 2009. Many olivine exposures are found in the concentric regions around South Pole-Aitken, Imbrium and Moscoviense impact basins on the moon where the crust is relatively thin. The olivine exposures could be an excavation of the lunar mantle at the time of the impacts that formed the basins (Pinet et al., 1993) or magnesium-rich pluton in the moon's lower crust. On the basis of radiative transfer modeling (Hapke, 2001; Lucey, 2004; Nakamura et al., 2009; Cahill et al., 2009), it is suggested that at least some of the olivine detected near impact basins originates from upper mantle of the moon. Olivine and orthopyroxene rich lithologies are observed exclusively in thin crust. Generally, in thicker crust (i.e.,>50 km), both olivine and orthopyroxene abundances are low (<15 to 20 vol.%). However, as the crust is less than 30 km thick, the abundance of these two minerals volume increases for many central peaks on the lunar surface (Cahill et al., 2009). It is thought that, the intermediate sized craters central peaks often possess olivine-rich materials, but the SP data showed that most of such craters central peaks did not have olivine. (www.jaxa.jp/press/2010/07/20100705_kaguya_e.html; Yamamoto et al., 2010). The finding of olivine along with thin crust has opened new space for researchers to explore whether it is excavated lower crust or upper mantle. The global distribution of the olivine concentration map is illustrated in the Fig.1.

3.1.2. Global distribution of pure anorthosite (PAN)

The composition of lunar highland crust is important for understanding the formation of global Magma Ocean hypothesis and subsequent evolution of the moon. The MI on the SELENE has a high spatial resolution of optimized spectral coverage, permitted to evaluate the composition of lunar crust. The MI has both visible and near-infrared coverage (Ohtake et al., 2008) with spectral bands at 415, 750, 900, 950 and 1000 nm (VIS) and 1000, 1050, 1250 and 1550 nm (NIR). The instrumental spatial resolution is 20 m (VIS) and 62 m (NIR) per pixel at the nominal altitude (100 km). Since, lunar surface soils regionally suffers heavily from vertical and lateral mixing due to processes of impact craters, crustal materials examination can be made at locations which are not subjected to extensive mixing (Tompkins and Pieters, 1999; Hawke et al., 2003). Ohtake et al. (2009) have focused globally distributed mixing-free younger craters and basins through their high reflectance. e.g: Jackson, South Ray, Tycho, Tsiolkovsky, and the northern and eastern portion of the Inner Rook Ring of the Orientale basin. Using ground based spectroscopy, it is proposed that a global anorthosite layer exists within the lunar crust and derived evidence for the presence of anorthosites in some locations on the moon (Hawke et al., 2003).

Based on the above findings, it has found that a strong correlation exists between the distribution of the pure anorthosite (PAN) rocks and the size of the craters. PAN rocks found in the craters that has diameters exceeding 30 km, whereas less feldspathic rocks in some craters has diameters smaller than 30 km. The excavation depth of a 30-km diameter crater is 3 km and considered that a global layer of PAN rock may exist within the upper crust, ranging from 3 km to 30 km in depth. The upper limit for the possible PAN rock layer could be shallower than 3 km because our observation provided only the maximum depth for the upper limit. The global PAN rocks were probably formed by the crystallization and segregation of plagioclase from lunar magma ocean of the moon and thus supports the existence of such a LMO (Ohtake et al., 2009). On the Earth, the purest anorthosite is produced by deformation (Lafrance et al., 1996). The anorthosites on the Earth could be reworked and tectonically modified remnants of an original widespread early anorthositic crust. Hence, Ohtake et al. (2009) suggested that, 'considering the extremely high plagioclase abundance, similar to the Earth's purest anorthosite, PAN rocks might also be generated by deformation. As the Giant impact hypothesis is mostly accepted by lunar scientists with the results of volatiles, isotopes and iron concentration gives better comparison with other hypotheses such as fission, capture, and co accretion. The Giant impact hypothesis supports the lunar magma ocean theory, so we can draw some conclusion about origin of PAN rocks from these hypotheses. Later work on lunar petrogenesis will discriminate the understanding of the formation of PAN rocks.
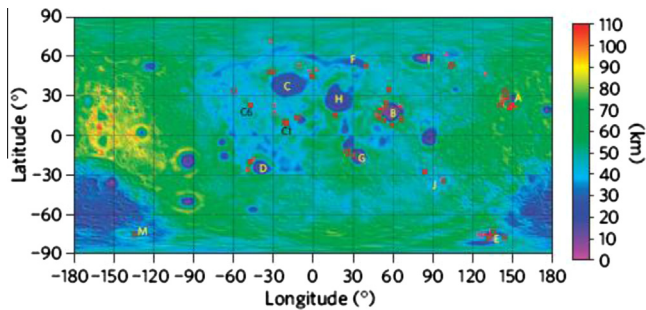
Fig. 1. Global distribution of olivine-rich points on the moon (after Yamamoto et al., 2010). The background map is the total lunar crustal thickness (crustal materials and mare basalt fills) based on SELENE gravity and a topographic model produced by the Kaguya explorer. The red squares indicate olivine-rich points. Note that most of the olivine-rich points are distributed around impact basins. The SP successfully detected olivine at the Copernicus (C1) and Aristarchus (C6) craters, which were identified as olivine-bearing areas by Earth-based observation.

3.1.3. Long-lived volcanism on the lunar farside

Volcanic history of the moon is important to understand the lunar origin and evolution. However, it is very difficult to get precise age of mare deposits due to a few lunar samples returned by Apollo or the lack of high spatial resolution images, particularly in farside. The SELENE provides a unique opportunity to map the whole lunar surface using Terrain Camera (TC) with 10 m/pixel to determine the model ages of mare deposits on the moon based on the crater size frequency distributions (CSFD). From high resolution TC images, it has found that, most mare volcanism on the lunar farside stopped before ~3.0 billion years ago, while a few mare deposits stopped before ~2.5 billion years ago (Haruyama et al., 2008). Recent missions Chandrayaan-1 (TMC-5 m/pixel) and LRO (LROC-NAC – 0.5 m/pixel) provide higher spatial resolution than the TC images. These fully calibrated TMC and LROC images will delineate the further interpretation on the lunar surface features.

3.1.4. Detailed farside lunar gravity field

The lunar gravity field play pivotal role in understanding the structure and the evolution of our celestial neighbor. The moon in the state of synchronous rotation made difficult to obtain detailed information of the "global" lunar gravity field. Lunar surface gravity at the equator is 5.32 ft/sec^2 (1.622 m/sec^2), nearly 1/6 Earth's gravity of 32.174 ft/sec^2 (9.806 m/sec^2). The lunar gravity field is uneven due to mass concentrations variations in the near and far side. The farside lunar surface never been directly observed by lunar missions. Analysis of the gravity field is an important criteria for the investigation of the interior of the moon. Except farside, the lunar gravity is measured through 2-way Doppler tracking orbiting the moon which is having low- sensitivity. SELENE measured the far side gravity field by 4-way Doppler measurement with a round trip communication between the Earth and the main orbiter on the far side through a relay satellite. Simulations

suggest that the new gravity model will be more accurate than the present models. The SELENE team developed a lunar gravity field model by using the tracking data of SELENE and Okina as a sub-satellite to improve the orbit determination, prediction accuracy and for the scientific analysis of lunar interior structure analysis. Based on this, Free-air Gravity Anomaly Map and Free-air Gravity Anomaly Error Map was created by Matsumoto et al. (2010). Namiki et al. (2009) proposed a new classification of the basins on the farside and limb based on the high magnitude of central gravity in free air anomaly compared to that of Bouguer anomaly. The SELENE models more greatly resolved the gravity of the farside by computing the correlation between gravity and topography. The high and low anomalies of spherical harmonic solution of the lunar Gravity Model (SGM100 h) is 695 and −730 mGal located at (32°E, 85°S) and (273°E, 80°S), respectively measured by SELENE (Matsumoto et al., 2010).

Matsumoto et al. (2010) described in detail the SELENE lunar gravity mission (SGM), including the tracking data acquisition and methodology to derive new spherical harmonic model of the SGM100 h, with emphasis on the 4-way Doppler data which have filled in most of the tracking data gap in the farside. As a result, SGM100 h, complete to degree and order 100, has been developed by incorporating the historical tracking data of the Lunar Orbiters, Apollo subsatellites, Clementine, SMART-1, Lunar Prospector and 14.2 months of SELENE Doppler range data including all the usable 4-way Doppler data. Compared to the 100th degree lunar gravity model from LP100 K, SGM100 h reveals greater detail in the farside free-air gravity anomalies which have larger correlations with the SELENE, laser altimeter derived topography (Araki et al., 2009). Correlations between gravity and topography can give insight into the planet's state of compensation (Watts, 2001). Based on this, Ishihara et al. (2009) computed lunar crustal thickness globally and confirmed that the crust below the Moscoviense basin on the farside is extremely thin. Ishihara et al. (2011) propose 'Double Impact Hypothesis' for the origin of Moscoviense basin using SELENE topographic map of Moscoviense basin which has triple and offset ring structure.

Sugano and Heki (2004) produced a High-resolution nearside gravity map by solving discrete mass anomalies without placing any priori power law constraint, to exhaust the gravity information contained in the LP Doppler tracking data. Han (2008) solved localized spherical harmonics to represent high-resolution gravity field over four selected spherical cap regions on the nearside. The approach of Han et al., (2009) was used to make power low constraint which is effective only within the farside and the limb region and able to get higher correlation with topography in the nearside only by using these techniques. However, the large farside data gap remained as a major challenge for global lunar gravity field modeling before the SGM90d which clearly resolved ring shaped farside gravity signatures within major impact basins.

3.2. Results from Chang'E-1

China's Chang'E-1 Lunar Orbiter was launched by China National Space Administration (CNSA) on 24th October 2007, as part of the first phase of the Chinese Lunar Exploration Program which aims to study the lunar environment and 3-D surface topography. The scientific goals of the Chang'E-1 are to obtain topography, geologic units of the lunar surface, tectonic out lines and to identify the future soft landing on the moon using global 3D stereo images (Ouyang et al., 2010; Lucey et al., 2000; Haruyama et al., 2009; Pieters et al., 2009; Ono et al., 2009; Namiki et al., 2009). γ-ray (GRS) and X-ray spectrometer (XRS) data were used to retrieve the abundance of the rock forming elements, map the major rocks and minerals to evaluate the important resource of the moon (Ogawa et al., 2008; Crawford et al., 2009; Grande et al., 2009). A multi-channel microwave radiometer is used to measure the brightness temperature (TB) of the moon to derive the thickness of lunar regolith and estimate the resource amount of helium-3 (Zheng et al., 2005; Haruyama et al., 2008; Ohtake et al., 2009). High-energy particle detector and solar wind ion detectors used to detect the space environment near the moon, including temporal and spatial variation on the composition, flux and energy spectrum of solar wind which could be useful to study the effect of solar activity on the Earth and moon (Ouyang et al., 2010). Chang'E-1 Interference Imaging Spectrometer (IIM) completed 84% coverage of the lunar surface between 70°S and 70°N.

Chang'E-1's GRS, IIM and XRS have achieved the abundance of some key elements and distribution of major minerals of the moon (Ouyang et al., 2010). Liu et al. (2010) characterized the Ti spectral features including Full Width Half Maximum (FWHM), absorption position, depth, area and symmetry using Chang'E-1 IIM images, RELAB spectra and Lunar Soil Characterization Consortium (LSCC) data. The IIM data with GRS used to detect the chemical and mineralogical compositions of the lunar surface (Zheng et al., 2008; Ling et al., 2011). Ling et al. (2011) developed a new algorithm to map TiO_2 abundance using Chang'E-1 IIM data, and then validated with the results of Apollo 16 landing site samples, and Clementine UVVIS-derived TiO_2 data. Highland and mare regional studies suggested that the TiO_2 map has good correlation with Clementine UVVIS results in corresponding areas. Based on these results, we can outline the distribution of KREEP rocks, mare basalt and highland plagioclase. Further, we can also develop fine tectonic map based on Chang'E-1 data in the future.

The global lunar topographic model and lunar digital elevation model with 3 km spatial resolution were obtained using laser altimeter data from Chang'E-1 (Li et al., 2010). The first two months data of Chang'E-1 with careful calibration were used to produce a global topographic map of the moon with a vertical accuracy of approximately 30 m and a spatial resolution of ~7.5 km (Su et al., 2011).

Topographic maps of the moon from Chang'E-1 (A) and SELENE Laser Altimetry (B) and LRO LOLA (C) are shown in the Fig. 2 This Chang'E-1-derived topographic map has a little higher spatial resolution than one from SELENE.

The global inventory of helium-3 in lunar regolith was estimated using data from the Chang'E-1 multi-channel microwave radiometer (Fa and Jin, 2010). Meng et al. (2010) attempted to calibrate data from the microwave radiometer and gained insights into mapping the water ice content in the Cabeus crater. Moreover, the composition of lunar surface materials, distribution of the elements, minerals and rock types on the moon were also obtained from Chang'E-1. Solar Wind Ion Detectors (SWIDs) on the Chang'E-1 observed two continuous flux peaks, without exceeding the prevailing solar wind proton energy and indicated that, existence of a pickup ion species is $m/q = 2$. The analysis showed the first evidence of H^{2+} ions in the lunar exosphere, which may provide the new insights of the evolution of solar wind hydrogen in the solar system (Wang et al., 2011). Thus, the Chinese Chang'E-1 lunar orbiter data have contributed to significant scientific outcomes such as global topography, estimation of rock forming elemental abundance, distribution of KREEP, basalts and anorthosites, characterization of Ti parameters and first evidence for H^{2+}, ions in the lunar exosphere.

3.3. Significant findings of Chandryaan-1

Chandrayaan-1 was India's first unmanned lunar probe. It was launched by the Indian Space Research Organization (ISRO) in 22nd October 2008, and operated until August 2009. The data captured by Chandrayaan-1 payloads gave new insights on lunar science including OH/H_2O, Spinel from Moon Mineralogical Mapper (M^3), Polar ice detections by mini-RF and uncollapsed lava tubes from Terrain Mapping Camera (TMC). The significant findings of Chandrayaan-1 are discussed in this manuscript apart from the other studies of geology, composition and topography of the moon.

3.3.1. OH/H_2O (Lunar water)

Lunar samples collected from Apollo and Luna programs left us with a belief that the moon is quite dry since the return of lunar samples from the Apollo and Luna programs. However, later explorations proved accumulation of volatiles, such as water frost and ice, could be possible in the permanently shadowed regions (PSR) of the lunar poles (Watson et al., 1961). Recent missions are trying to look for H over the lunar surface. For example, the H over the lunar surface and higher abundance was directly measured in the PSR of both poles by Lunar Prospector (LP) neutron spectrometer (Feldman et al., 1998, 2001), which indicates that polar regions are potential cold traps for volatiles (Crider and Vondrak, 2002) and could be linked to solar-wind hydrogen (Starukhina and Shkuratov, 2000). Trace water or minor hydrous minerals were observed in

(A) Topographic map from Chang'E-1

(B) Topographic map from SELENE
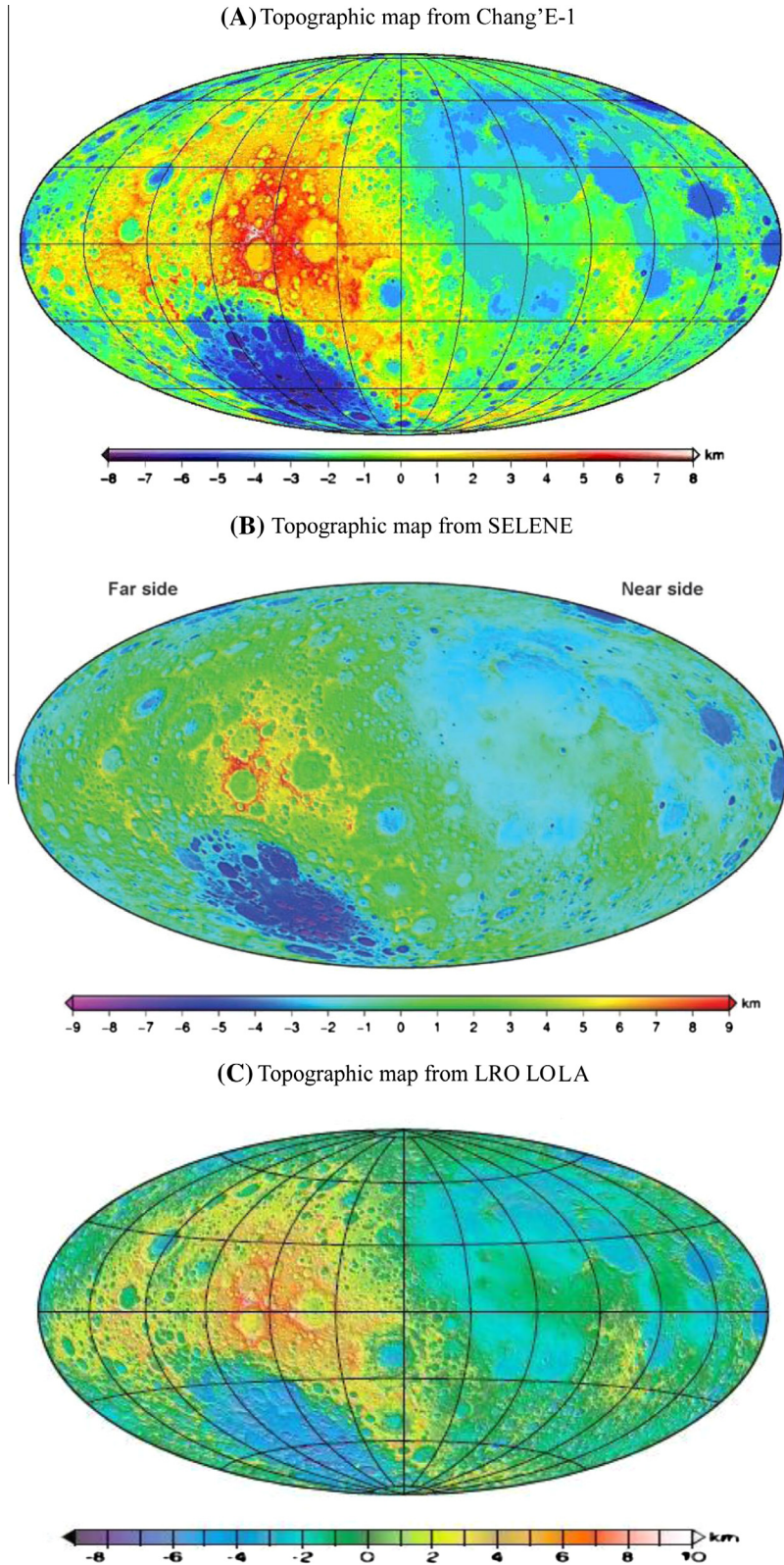

(C) Topographic map from LRO LOLA

Fig. 2. Topographic maps of the moon from Chang'E-1 (A) (after Su et al., 2011), SELENE Laser Altimetry (B) (after Araki et al., 2009) and LRO Laser Altimetry (C) (after Smith et al., 2010a, b).

many Apollo samples, but these have typically been attributed due to terrestrial air contamination. Highly sensitive secondary ion mass spectrometry (SIMS) detected

20 – 45 ppm trace water from the interior of Apollo 15 and Apollo 17 Orange volcanic glasses, which are considered as most primitive materials from the lunar mantle

(Saal et al., 2008). The mini-radio-frequency (mini-RF) radar mounted in Chandrayaan-1 was the first polarimetric synthetic aperture radar (SAR) outside Earth orbit (Goswami and Annadurai, 2009) and it mapped over 95% of the lunar poles (latitude > 80°) at 150 m radar resolution (Spudis et al., 2010). The ice at the Polar Regions was found by Mini-SAR, implying that ice is heterogeneously distributed in the small craters near the North Pole. The young primary impact craters have higher (>1) Circular Polarization Ratio (CPR) imply that surface roughness associated with fresh craters. Some craters in the North Polar show elevated CPR in their interiors only in the permanent shadowed places which have correlation with proposed locations of polar ice modeled by LP. The surface roughness and higher CPR ratio relations are consistent with deposits of water ice in the polar region craters (Spudis et al., 2010).

M^3 measurements reported that, evidence of widespread OH and H_2O in the lunar surface layer (Pieters et al., 2009). The absorption at 3 μm data indicates a minor hydrated phase or hydration process occurred on the lunar surface which means that, moon contains primary hydrated mineral phases. The significant amounts of mobile water in the higher latitudes of the moon may provide source for the polar ice inferred from these measurements (Pieters et al., 2009). But the accumulation of volatiles, including water frost and ice in the PSR of the lunar poles still remains undisclosed. The absorption at 2.8 to 3 μm from M^3 coverage reveals OH and H_2O features (Pieters et al., 2009). LP neutron spectrometer found that, Hydrogen spreads about 0.5 m on the surface in the polar regions (Feldman et al., 1998, 2000, 2001). This finding leads the science communities to a conclusion that, water might be cold trapped and stored for long time periods in PSR to several meters in depth and gardened to nearer to the surface by impacts (Watson et al., 1961).

Evidence of water ice and other volatile materials (Colaprete et al., 2010) were reported by Lunar Crater Observation and Sensing Satellite (LCROSS) experiment at shadowed part of a lunar polar crater. Lucey (2009) suggested that the potential water on the moon are possibly from in-fall of meteorite and cometary bodies, original material during formation of the moon or produced from interaction of solar wind and surface material. The strong 2.8 and 3 μm absorptions are considered as OH/H_2O features, which are observed only in the highland regions of the lunar surface. These features are weak and almost absent in the mare regions and these differences remains unclear (Pieters et al., 2009). Graham et al. (1979) suggested that adsorbed water in mare materials is released at lower temperatures than adsorbed water in highland materials which is consistent with stronger absorption bands at 2.8 μm and 3 μm on fully illuminated highland surfaces than on fully illuminated mare surfaces. However, the variation might be due to observation bias also.

3.3.2. Uncollapsed lava tubes

The Terrain Mapping Camera (TMC) on Chandrayaan-1 provides panchromatic spectral range of 0.5–0.75 μm with a stereo images view in the fore, nadir and aft directions of the spacecraft movement, which enables three-dimensional viewing capability (Kumar et al., 2009). Digital Elevation Model (DEM) with 5 m resolution enables scientists to delineate the topographical variations on the lunar surface such as altimetry, areal extent and gravity measurements. These are essential parameters to create DEM, Digital Terrain Model (DTM) and measurement of crater diameter, depth and areal extent, mare basalts extension, multi ring basin studies. Arya et al. (2011) identified a largest 140 m diameter and 360 m cross sectional portion and thickness varies from 45–90 m uncollapsed lava tube which could be a probable site for human habitability for future human lunar missions and scientific explorations, providing a safe environment from hazardous radiations, micro-meteoritic impacts, extreme temperatures and dust storms. The previous missions also identified smallest uncollapsed and collapsed lava tubes on the lunar surface. The human settlement on the moon is very difficult due to absence of an atmosphere and intrinsic magnetic field make the lunar surface vulnerable to impacts of meteorites and other bodies as well as energetic particles and radiations. The identified underground lava tube is the uncollapsed portion between the two rilles located in the Oceanus Procellarum, to north of Rima Galilaei above the lunar equator and could be suitable for astronaut during human spaceflight program. Apart from this, TMC data could also be used in the selenomorphological studies, crater counting for chronological study and topographical variation between mare and highland regions.

3.3.3. New rock spinel

Mg-rich spinel with no other mafic minerals detectable (<5% pyroxene, olivine) called as "OOS" since they contains orthopyroxene, olivine and spinel were identified on farside Moscoviense Basin and considered as new composition that has not been recognized in lunar samples and is new for lunar science community. The rock is consistent with a spinel- anorthosite assemblage and contains more Mg–Al rich spinel (not chromite) and represented components of deeper crust uplifted and exposed by the basin-forming event itself. M^3 has identified a suite of highly unusual rock types with no detectable absorption feature near 1000 nm but exhibits a prominent absorption centered near 2000 nm (Fig. 3) (Pieters et al., 2011). Distinctive NIR spectral properties have not been seen in remote measurements and have only been observed for isolated small lunar Mg–Al spinel as studied in thin section (Mao and Bell, 1975). The dark and bright spinel, orthopyroxene and olivine-rich lithologies in the Integrated Band Depth (IBD) of 1000 image indicates that space weathering is insufficient to erase or hide small exposures of unusual rock-types of OOS for billions of years (Pieters et al., 2011). Currently available high spatial and spectral data helps to delineate the similar exposures of material across the entire surface of the moon. The detection and characterization of OOS demonstrate the Moon's compositional record and geologic

context in more detail with modern tools. It is inferred that, there are cases where the spinel is spatially close to the orthopyroxene lithology and where the orthopyroxene occurs in close nearness to the olivine lithology suggesting they may be genetically linked.

3.3.4. Global and olivine concentration

The high resolution images and their spectral profile characteristics provided opportunity to determine even scanty minerals and elements on the lunar surface. The recent SELENE (SP) and Chandrayaan-1 (M^3) images were utilized to identify the global olivine concentration on the lunar surface by Yamamoto et al. (2010) and Isaacson et al. (2011). The compositional diversity was observed in the olivine rich sites from a small crater through visual evaluation of the olivine spectra. Spectrally homogeneous olivines were found from Copernicus, which were compositionally more homogeneous than those from Moscoviense olivine. Furthermore, Aristarchus and Marius olivine have clear spectral differences from Moscoviense and Copernicus, suggesting possible contributions from other phases also (Isaacson et al., 2011). Aristarchus has absorptions at 1050 and 1300 nm due to olivine and plagioclase or Fe-glass respectively. Since, Fe- glass is not observed in this region, the 1300 nm absorption is only due to olivine and plagioclase mixture.

Olivine has identified in the Aristarchus, Marius, Moscoviense and Copernicus based on 1000 nm absorption feature. The Moscoviense and Copernicus olivine spectra shows strong similarity and they have different ratios in Fe:Mg concentration. Aristarchus spectrum shows 1300 nm absorption due to Plagioclase (Fe) and it shows mixture of olivine and Plagioclase suggests that this olivine is product of melted basaltic source associated with impact melt-derived materials. Marius spectrum shows 2000 nm absorption feature may be due to chromite/pyroxene. Modified Gaussian Model (MGM) is used to quantify the olivine dominated spectra in all these four regions. Copernicus olivine shows homogeneity in their region but Moscoviense olivine has slight spectral variation and shows composition diverse in the Moscoviense region. Aristarchus olivine has long wavelength (1300 nm) absorption and Marius olivine has 2000 nm absorption means that it has different lithological association (contamination) compared to Moscoviense and Copernicus olivines (Fig. 4). In Aristarchus and Marius contaminations suggest that, the two regions are not having genetic relationships as well as they were formed with different geological process.

3.3.5. Characterization of mare basalts

Based on the chemical composition, mare basalts are divided as two broad groups as, older high-Ti group (age 3550 to 3850 million years, TiO_2 content 9–13%) and the younger, low-Ti group (age 3150 to 3450 million years, TiO_2 content 1–5%). Low and High -Ti basalts are probably derived from an olivine-pyroxene source rock at depths ranges from 200 to 500 km and olivine-pyroxene-ilmenite

cumulates in the outer 150 km of the moon respectively (Papike et al., 1976). Lunar Liquid Oxygen (LLOX) could be produced by reduction of raw immature-sub mature mare soils and basalts. Chambers et al. (1995) successfully used the Apollo returned basaltic samples to produce the LLOX. Now it is attractive for LLOX production due to High-Ti mare soils unconsolidated nature, high ilmenite abundance and widespread distribution. The ilmenite concentration (∼10–20%) of high-Ti mare rocks and soils makes these materials ideal for hydrogen reduction to produce LLOX. In the future, if we want to establish the lunar base, LLOX is necessary to use as fuel oxidant and for life support. Hence, there is a need to identify the potential regions of high-Ti basalts in the nearside of the lunar surface.

Linear Spectral Unmixing (LSU) is to determine the relative abundance of materials that are represents in multi-spectral or hyperspectral imagery based on the materials' spectral characteristics. The reflectance at each pixel of the image is assumed to be a linear combination of the reflectance of end member present within the pixel. LSU is a commonly accepted approach to mixed-pixel classification in hyperspectral imagery. The RELAB spectra of lunar minerals and Clementine UVVIS-NIR data were used to establish the olivine, clinopyroxene, orthopyroxene, plagioclase and ilmenite abundance map of the lunar surface based on linear spectral unmixing (Bokun et al., 2010). In the present study, end members are selected from the bidirectional reflectance spectra of low, medium and high – Ti basaltic soils with various grains from RELAB facility. The spectral values are averaged for the various grain sizes and one spectral end member derived for each basaltic soil established for low, medium and high Ti-mare basalts. The RELAB basaltic end members and 3 mare test site basalts spectra were compared (Fig. 5). Since, the reflectance information may be complicated due to thermal emission signatures at longest NIR wavelengths beyond 2.6 μm those were not used in this study. Hence, spectra and spectrally subsetted M^3 data from 450 – 2500 nm were used to estimate the abundance of the various basalts in the Orientale basin basaltic terrain.

In the present work, parts of basaltic regions from Mare Orientale, Lacus Veris and Lacus Autumni of the Orientale basin is studied with help of Moon Mineralogical Mapper (M^3) data of Chandrayaan-1 orbiter. The spectral profiles and LSU techniques are attempted to characterize the various basalts such as low, medium and high-Ti basalts in the Mare Orientale basin and compared with RELAB basaltic spectra. The RELAB averaged chemistry and spectral data of low (15071), medium (12030) and high (71501) – Ti basalts were taken as the end member for analysis. The distribution and nature of TiO_2 basalts in the Orientale basaltic regions were analyzed in quantitative manner. The low, medium and high - Ti basalts concentrations map was established for the Orientale region (Fig. 6). The results are consistent with RELAB and conventional analysis. Through this study, it is found that, the mare Orientale has high-Ti basalts compared to the nearest Lacus
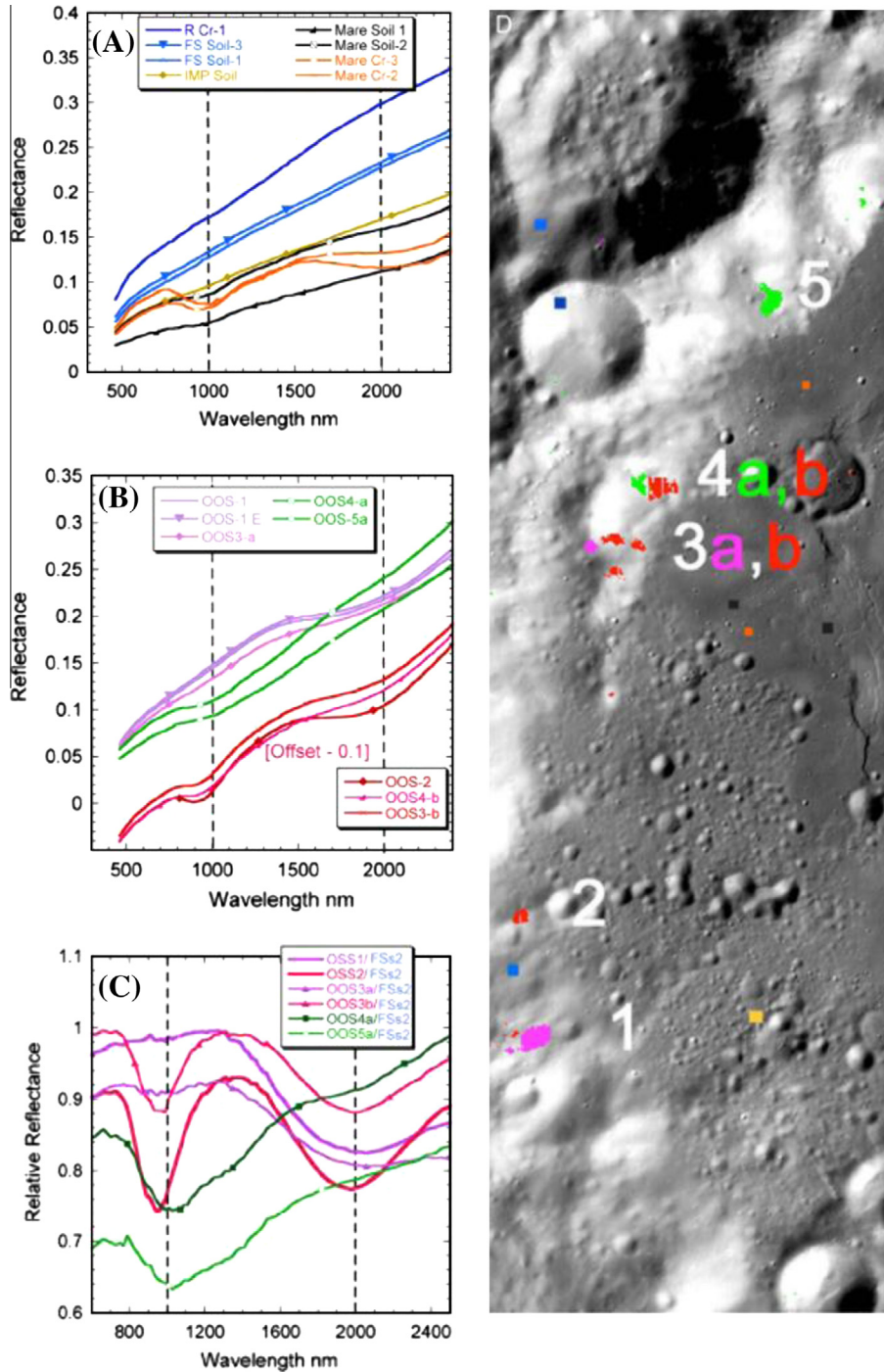
Fig. 3. M3 spectra of OOS regions: (A) Apparent reflectance of local basin materials; (B) apparent reflectance of OOS regions; (C) relative reflectance spectra of OOS relative to a local featureless soil of similar albedo (blue in figure a); (D) The locations of OOS (after Pieters et al., 2011).

Autumni and Lacus Veries. With the fully calibrated M^3 data, we could able to characterize basalts globally in the lunar surface. This task possesses a new challenge in lunar studies.

3.4. New findings from Lunar Reconnaissance Orbiter (LRO)

Lunar Reconnaissance Orbiter (LRO) is leading NASA's mission and the primary objective of LRO is to conduct investigations that prepare for future lunar exploration, e.g., inspecting safe and compelling landing sites, locating potential resources, looking for the possibility of water ice and characterizing the effects of prolonged exposure to the lunar radiation environment. Although the SELENE and ChangE-1 provided high resolution topography, there are still limitations in accuracy and resolution. The LRO provided rich scientific data for better understanding of lunar composition and topography. For example, the previously undetected lobate thrust-fault scarps
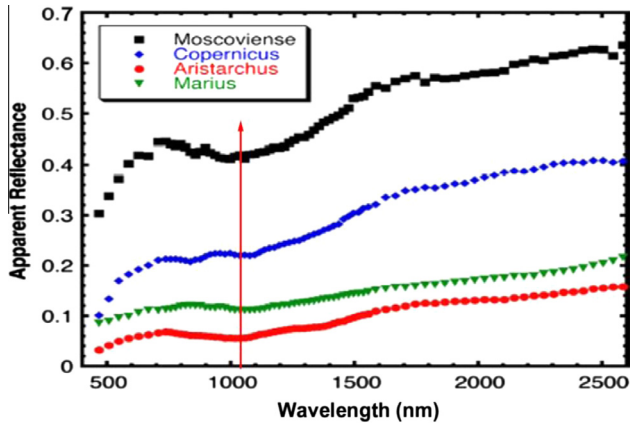
Fig. 4. Example M3 spectra of typical olivine rich sites collected from Moscovience, Copernicus, Aristarchus and Marius regions (after, Isaacson et al., 2011).

and associated meter-scale secondary tectonic landforms were revealed by Lunar Reconnaissance Orbiter Camera (LROC) images (Watters et al., 2010), including narrow extensional troughs or graben, splay faults, and multiple low-relief terraces. Also the most detailed characterization of the morphology and relief of lunar lobate scarps were obtained from high resolution topography derived from Narrow Angle Camera (NAC) on LRO with a scale as low as 0.5 m/pixel (Robinson et al., 2010).

The Lyman Alpha Mapping Project (LAMP) ultraviolet spectrograph from LRO observed the plume generated by the Lunar Crater Observation Sensing Satellite (LCROSS) impact as far-ultraviolet emissions from the fluorescence of sunlight by molecular hydrogen and carbon monoxide and resonantly scattered sunlight from atomic mercury, with contributions from calcium and magnesium (Gladstone et al., 2010). The objectives of the LAMP investigation are (a) search for exposed water ice near the lunar poles and in PSR using reflected Lyman-Alpha (b) sky-glow and far-ultraviolet starlight, (c) landform maps in the PSR regions which serve as pathfinder for lunar natural light night vision system (d) Obtain data on the tenuous lunar atmosphere (Chin et al., 2007). The light curve from

LAMP is completely consistent with the immediate formation of H_2, and substantial contribution of H_2, from the photolysis of water is exempted by the strict upper limits on other photolysis products, e.g., H and O. LCROSS mission designed to provide evidence on water ice which may present in permanently shadowed craters of the moon. On 9 October 2009, a spent Centaur rocket struck the PSR within the lunar South Pole crater Cabeus, ejecting debris, dust, and vapor, which was observed by a second "shepherding" spacecraft. Water vapor, ice and ultraviolet emissions attributable to hydroxyl radicals support the presence of water in the debris recognized by NIR absorbance. Light hydrocarbons, sulfur-bearing species, and carbon dioxide were observed along with water (Colaprete et al., 2010).

The Lunar Orbiter Laser Altimeter (LOLA), a payload element on NASA's LRO (Chin et al., 2007). The objective of the LOLA investigation is to characterize potential future robotic or human landing sites and to provide a precise global geodetic grid of the moon. Also LOLA offered surface slope, surface roughness and reflectance as ancillary measurements. The radial accuracy of the LOLA's global topographic model is < 1 m (Fig. 2C) and the spatial accuracy of the lunar geodetic grid is ∼30 m (Smith et al., 2010a, b). The maps produced by using high resolution LOLA data definitely help the future lunar projects for selecting precise landing locations.

Diviner Lunar Radiometer Experiment (DLRE) on the LRO provided global coverage maps of thermal-infrared derived compositions on the moon for the first time in lunar exploration history. Since infrared emission spectroscopy is sensitive to the bulk composition, important lunar silicates can be readily identified, such as feldspar, pyroxene, olivine, and quartz (Salisbury and Walter, 1989). The DLRE compositional investigation relies primarily on the three shortest wavelength thermal infrared channels near 8 μm : 7.55 to 8.05 μm, 8.10 to 8.40 μm and 8.38 to 8.68 μm. These observations are consistent with previous regional lunar surface observations and comparable with laboratory measurements of returned lunar rocks and soils in a simulated lunar environment (Murcray et al., 1970).
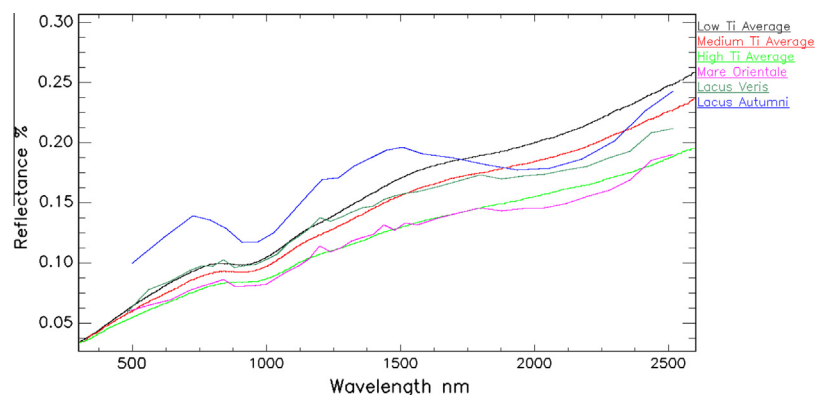

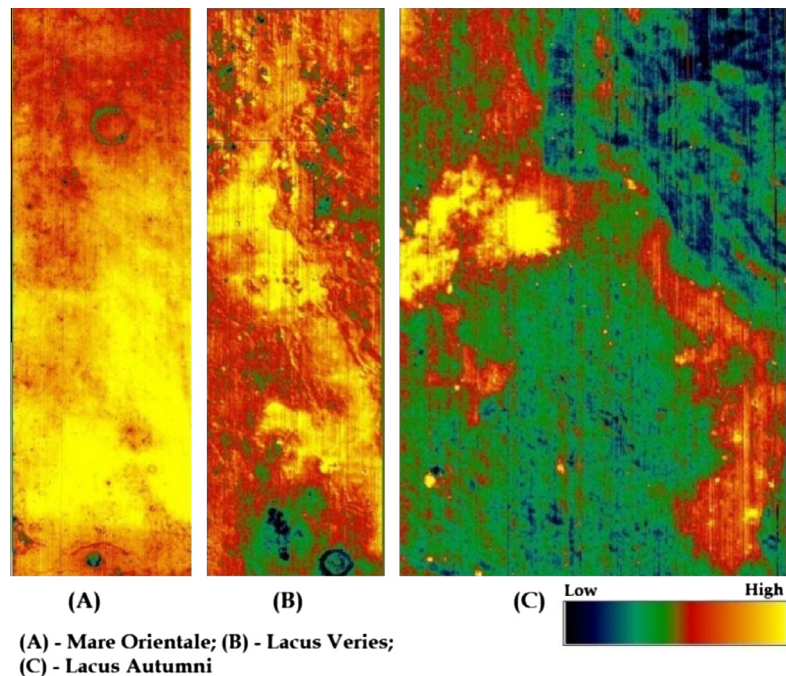Fig. 5. Low, medium and high Ti basalts spectra with test site spectra.

(A) - Mare Orientale; (B) - Lacus Veries;
(C) - Lacus Autumni

Fig. 6. The low and High Ti basalts characterization using M3 and RELAB spectral data.

DLRE 8 μm region spectra used to determine the maxima of parabolic fits ("Christiansen Feature (CF) values") and assemble the result into a comprehensive map of lunar silicate mineralogy. Over 90% of the CF values are located in between 8.04 and 8.36 μm. The mineralogical differences between maria with abundant pyroxene and the highlands with rich plagioclase feldspar are readily noticeable based on the CF (Fig.7) (Greenhagen et al., 2010). Glotch et al. (2010) used DLRE data to perform a comprehensive survey of the lunar red spots and identified Hansteen Alpha, Lassell Massif, the Gruithuisen Domes, and Aristarchus Crater as high silica features and suggested that, basaltic intrusive magmatism may have remelted and subsequently differentiated a previously more silica-rich precursor, such as anorthositic crust.

Mini-RF is a lightweight Synthetic Aperture Radar (SAR) on NASA's LRO operated at either 12.6 or 4.2 cm wavelength with 7.5 m/pixel spatial resolution and ~18 km and ~6 km swath, respectively. The objectives of Mini-RF are a) to image the land form scale of the permanently shadowed craters; b) to search for ice deposits; c) to provide information on meter-scale features of the Constellation landing site list; d) to acquire global topographic information; and e) to characterize lunar mineralogy. Mini-RF has acquired good quality of data with radar backscatter properties of the lunar surface. Thomson et al. (2011) reported Mini- RF observations of 20 km diameter Shackleton crater situated at inner rim massif of the much higher South Pole-Aitken Basin. LCROSS impact nearby Cabeus region (Colaprete et al., 2010), and Lunar Prospector as well as LRO's Lunar Exploration Neutron Detector (LEND) suggested polar concentrations

of excess hydrogen (Lawrence et al., 2006; Mitrofanov et al., 2010). Mini-RF remains a viable candidate site of polar volatile accumulation when viewed in conjunction with other data like DIVINER (Paige et al., 2010).

4. Evaluation of main payloads and results

Among the stereo imager data from Chang'E-1, SELENE, Chandrayaan-1 and LRO missions, the LRO's NAC provides 0.5 m spatial resolution imagery which is very much useful in terms of lunar chronology through crater counting, undetected lobate thrust scarps and associated small scale tectonic landforms and characterization of lunar topography and morphology. The TMC on Chandrayaan1, which is having 5 m spatial resolution data have extensively used to locate the un-collapsed lava tubes, surface age determination and topographical studies by creating DEM and DTM. The Terrain Camera on SELENE and Stereo Camera (SC) on Chang'E-1 have spatial resolution of 10 m and 120 m respectively. The TC data are also used to derive the modal ages of the lunar surface through crater size frequency distributions (CSFD) and the SC data used to develop the 3D stereo images to outline the topography, geologic units and tectonic outline graph of the lunar surface.

Among the recent four missions, Chang'E-1 and SELENE were equipped with VNIR multispectral camera and Chandrayaan1 equipped with VNIR hyperspectral sensor. The primary objective of the VNIR sensors is to retrieve the lunar surface chemical composition. HySI has 64 contiguous bands where Chang'E-1 and SELENE have 32 and 9 multispectral bands respectively. The data from
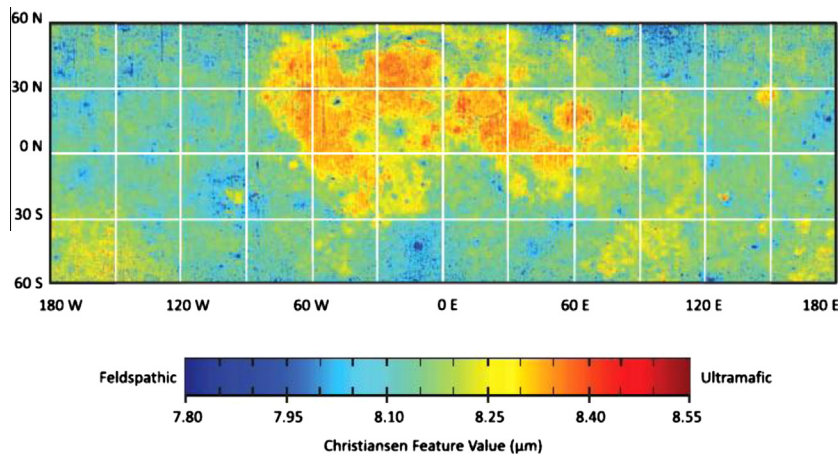
Fig. 7. CF value map of silicate mineralogy (after Greenhagen et al., 2010).

VNIR sensors were used to estimate FeO, TiO_2 concentrations globally. The MI on SELENE has given the global distribution of PAN with the absorption feature at 1250 nm. Due to lower spectral resolution of HySI and IIM further analysis are limited when compare to the currently available recent data sets.

SELENE and Chandrayaan-1 missions were equipped with IR hyperspectral spectrometers such as Spectral Profiler (SP) and moon Mineralogical Mapper (M^3) respectively. SP has spectral resolution of 0.5 μm – 2.6 μm region with the spatial resolution of 500 m/pixel. The M^3 has spectral resolution of 0.45 μm – 3 μm and the target mode spatial resolution is 70 m/pixel and global mode spatial resolution is 140 m/pixel with the swath of 42.5 km. The important result obtained from SP is global distribution of olivine in the lunar surface. Similarly M3 has identified OH/H_2O based on 3 μm absorption bands and Spinel mineral identification based on 2 μm absorptions.

Among the recent lunar missions, LRO orbiter has UV imager to provide spectrally finger print of exposed H_2O frost in the lunar Polar Regions. LRO has provided the technology with military night vision equipment using UV starlight and Lyman α sky glow as its light source, while Chang'E-1, SELENE and Chandrayaan-1 missions have X-ray spectrometers to measure the elemental abundances and map the distribution of the main rock forming elements, e.g., Mg, Al, Si, Ca, Ti and Fe with different energy range and spatial resolutions. Elemental composition is crucial in not only the geochemical nature of terrains on the lunar surface, but also the history of impact activity and volcano-tectonic episode of the moon. Chang'E-1 and SELENE posses GRS, with different energy ranges as well as spatial resolution. GRS is a special kind of instrument which is extensively used for remotey measuring the abundances of chemical elements like C, O, Mg, Al, Si, K, Ca, Fe, Th and U on the planetary surface.

Further, LRO is equipped with Neutron Detector (LEND) to measure the global distributions of neutron flux which are produced by the continuous cosmic ray with different energy bombardment on the lunar surface from thermal energy up to >15 MeV. The neutron detector already collected enormous data through onboard Lunar Prospector which proposed that the PSR bearing water ice deposits. The recent LRO results were also consistence with LP neutron detector.

All the recent lunar missions having laser altimeter with varied spectral and spatial resolution. The laser altimeter data are very much useful to construct digital elevation maps (DEM) of the lunar surface. Among the altimeter data, LOLA from LRO has provided the geodectic location, its direction and magnitude of surface slopes and the elevation variation at scales relevant to landing sites, surface mobility and surface roughness. Since the laser ranging (LR) data is used to determine three dimensional lunar geodectic grid, based on the precise seleno location of ground spots and LR provided the foundation for positioning data sets from their own and other lunar missions.

Plasma ion spectrometer is available in all recent missions with differenced energy level, spatial and spectral resolution is used to understand the environment of the moon. The plasma ion spectrometer data prove to be useful for observing lunar surface charging in response to solar and plasma environment, dust transport and dusty plasma exosphere, mapping of surface composition and volatiles. Through this it could be possible to derive basic space plasma physics and solar interactions with lunar surface. The target oriented lunar plasma observations are essential in order to develop essential discharge and dust mitigation strategies for future robotic and human lunar exploration. Sub-kV atom reflecting analyzer (SARA) and Radiation dose monitor (RADOM) are exclusively fixed in Chandrayaan1. SARA is used to detect the neutral atoms from the lunar surface and estimate the concentrations of H, O, Na, K, Ca & Fe atoms. RADOM is used to measure deposited energy from primary and secondary particles of solar and galactic.

Micro wave sounder with varied spectral and spatial resolution is used inevitably in the recent lunar missions. The

microwave sounder is mainly to focus PSR near lunar poles to look for signatures of water ice in the top meter of the lunar surface material. The Chandrayaan-1 and LRO's micro wave sounder have provided reliable data which were discussed in the earlier sections. DLRE has mapped global day and night time lunar surface temperature, to characterize thermal environments for habitability, to determine rock abundances and landing sites, to identify potential polar ice reservoirs and map variations in the silicate mineralogy. The Chandrayaan-1 and LRO missions have moon impact probe with the weight of 600 and 2300 kg respectively. The main objective of these impacts is to detect possible presence of trace gases, water molecules in the lunar exosphere in permanently shadowed locations near to the lunar South Pole during the impact and excavation.

5. Future objectives and scientific questions

5.1. Source for OH/H₂O

Out of 3 possible sources discussed in the section 3.3 about the presence of OH/H_2O on/in the moon, the 2.8 and 3 μm absorption bands favor solar-wind proton-induced hydroxylation as the source of OH and possibly H_2O. Water molecules from interior of the lunar samples is thought to come from deep (Saal et al., 2008) and appears not likely to exist in the widespread deposits mapped by M^3. The solar wind products are found in the lunar samples and associated with smaller grains of larger areas. The strong 2.8 and 3 μm absorptions are considered as OH/H_2O features observed only in the highland regions of the lunar surface and these features are weak and almost absent in the mare regions. For better understanding about OH/H_2O, M^3 spectra have drawn with various illuminated angle data for comparison.

Over 95% of the lunar poles were mapped (latitude > 80°) at 150 m radar resolution by Chandrayaan-1 Mini-SAR during February to April 2009 (Spudis et al., 2010). The LCROSS experiment impacted the Centaur upper stage rocket into a shadowed part of a lunar polar crater in October 2009 and evidence of water ice and other volatile materials (Colaprete et al., 2010) were reported. The Lunar Prospector neutron spectrometer directly measured H over the moon and found a higher abundance associated with the PSR of both poles (Feldman et al., 1998, 2001), implying that the lunar poles could be potential cold traps for volatiles (Crider and Vondrak, 2002) and some of which could be linked to solar-wind hydrogen (Starukhina and Shkuratov, 2000).

Prior to the M^3 discovery, the Lunar Prospector's neutron spectrometer observations interprets, excess hydrogen may present in the lunar polar regions within about 0.5 meters on of the surface (Feldman et al., 1998, 2000, 2001). Several scientists suggested that these results stands as an evidence that, water might be cold-trapped and stored for long time periods in PSR to several meters in

depth and gardened to nearer surface by impacts (Watson et al., 1961).

5.2. Spinel formation

The OOS compositional information about the lunar crust opens new avenues of inquiry like what are the initial compositions of melts that are needed to produce three lithologies? How and when was the melt formed? What materials were melted? From where, these materials excavated? How did the mineral separation and concentration occur at the scale observed? What was the size of magma chamber is needed to allow such clear separation of lithologies as a layered intrusive? What are the depth and temperatures? (Pieters et al., 2011). In order to answer questions, we need further petrological and petrogenesis analysis of available and future lunar collected near future.

5.3. Active volcanism on moon

The lunar samples obtained so far from all lunar missions collectively establishes the fact that, lunar volcanism was ceased about 3.2 billion years ago and the dead moon model is accepted widely. But degradation models and crater statistics indicate that last gasp effusions of thin basalt sequences may have extended to 1.0 billion years ago (Schultz et al., 2000). As on Earth, basalt is created by partial melting of mantle rocks, which is mostly composed of iron and magnesium rich minerals like olivine and pyroxene. Apollo 11 basalts are the first samples returned from moon (~3.8 B.Y), which reveals that the basalts are depleted in volatile content and have large amounts of titanium and iron. Basalts from other Apollo missions largely confirm the initial results but Apollo 12 basalts (3.1 B.Y) have lower titanium than the Apollo 11 and found that, 600 – 700 million years younger. The lower titanium and younger ages of the Apollo 12 basalts confirmed that, all the maria were not erupted as single phase. This is an extended process and different batches of magma erupted in different places and different times described the complexity in the volcanic history of the moon. The Mare Imbrium basin rim sample taken by Apollo 15 basalts have low-Ti and slightly older age (3.3 B.Y) than that of Apollo 12. The Mare Serenitatis basalts brought by Apollo 17 has very high-Ti basalts similar to Apollo 11 but slightly younger age (3.7 billion years). These results concluded that, moon had a fairly simple volcanic history, with early eruptions of high-Ti lava and late eruptions of low-Ti lava and suggests that the moon "died" volcanically after Apollo 12 lavas which erupted 3.1 billion years ago. The results are totally unwarranted that even today these facts are widely believed and recounted (Spudis, 2000).

The preservation state of small-scale relief, lightly cratered, result of episodic out gassing and lack of space weathering and associated with bright regions suggests that, the portion of INA is being less than 10 Myr old (Schultz et al., 2000). INA has 2.9 km in diameter and

30 m depth, with numerous smooth mounds and plateaus <10 m high, and surrounded by features like reflective, low-lying, rubbly plains. Soils surrounding INA has weak mafic band and 0.8 km diameter "western" crater exhibits a stronger band with no change in albedo indicating the presence of more mafic and/or less weathered materials. Schultz et al. (2000) suggest that the observations do not preclude the possibility that, it is still in the process of formation.

The morphology of the INA structure was revealed through recent LRO - Narrow Angle Camera (NAC) images with up to 0.5 m/pixel resolution (Robinson et al., 2010). The INA floor material displays the strongest mafic bands and optically immature mare craters in Mare Serenitatis and Mare Tranquillitatis (low and high-Ti mare basalts, respectively). For comparison, the least weathered 1% of mare materials were sampled from each basalt type based on the models of mare maturity (Staid and Pieters, 2000; Wilcox et al., 2005). In addition, relatively unweathered high- Ti basalts within the blocky floor materials in the INA structure was identified using M3 data have consistent with previous studies (Staid et al., 2011).

Schultz et al. (2006) found other three features similar to INA which is related to linear rilles associated with the Imbrium impact basin which may be places of crustal weaknesses that allow interior gases to escape. The INA structure has only 2 craters > 30 m diameter in the 8 Sq.km area and optical maturity plot also shows INA immaturity. Gas release won't be visible for more than second, but dust came up from surface may stand few seconds. Using the professional telescope if we can get a spectrum of the degases, it will very useful to identify the composition. The gases coming out of the moon might include H_2O (vapour), SO_2 and CO_2. Monitoring and exploring INA and similar structures from earth and form the upcoming lunar missions, we can get more insights about the nature of degases and these findings will establish their potential as a resource for future lunar exploration. With all these findings, one may end up with the question "Is the Moon alive?". If it alive, why it is not erupting?. Based on the conclusions arrived out of the lunar missions, it makes sense to think that the Moon is ALIVE. What we are sensing is now are the last gasps of the moon. (Schultz et al., 2006). So, the further research about INA and searching of similar features are good targets for future exploration. The best way to gain further knowledge about lunar origin and evolution is to collect soil samples from INA.

Images of the lunar surface show sinuous lava channels called rilles, and volcanic domes, cones and collapse pits. These features support the theory that, there was once active volcanism on the moon. However, large shield volcanoes (domes) and calderas are not observed on the moon. But small lunar shield volcanoes have summit pits in the 1–3 km diameter range (Head and Gifford, 1980), and there is little evidence for the presence of large circular caldera-like structures similar to those seen on the Earth, Mars and Venus (Head and Wilson, 1991). If we would know

the age of the last eruption, we could answer the question, when the moon "Shut down" thermally.

5.4. Tectonics of moon

The moon is the only extra terrestrial object studied extensively in all as aspects in the 21st Century including Structural geology. The finite deformation of lunar lithosphere is visualized by tectonic features such as wrinkle ridges and straight rilles and interpreted as anticlinal fold (Watters and Schultz, 2010). These features imply that the secular and spatial changes of the surface, boundary condition of stress that has been controlled by endogenic and exogenic processes. Such information not only limits our understanding on the mechanical properties of the lunar lithosphere, but also on the regional and global thermal histories and even on the origin of the Earth-Moon system (Atsushi et al., 1998).

Impact basins are found in tectonic landforms in and around the nearside lunar maria, such as wrinkle ridges, rilles and narrow troughs, which exclusively occur in mare basalts and margins of basins adjacent to highlands. The Lee – Lincoln scarp located on the Taurus- Littrow valley near to Apollo 17 landing site exemplifies an important class of lunar faults, lobate scarp thrust faults. The vast majority of the Moon's large scale tectonic features are found in the basalt-filled impact basins and the adjacent highlands (Watters and Johnson, 2010).

Wrinkle ridges are morphologically complex landforms that occur in mare basalts which were first discovered and mapped using Earth-based telescopic observations (Gilbert, 1893; Baldwin, 1965). Gilbert (1893) interpreted that, wrinkle ridges are anticline forms and later it has been interpreted as volcanic features related to the emplacement of the mare basalts or the result of intrusion or extrusion of lava into fractures and zones of weakness following crustal extension related to basin localized at global tectonic patterns (Quaide, 1965; Tjia, 1970; Hartmann and Wood, 1971) and others interpreted as mare ridges are purely tectonic landforms (Baldwin, 1965; Howard and Muehlberger, 1973). Apollo Lunar Sounder Experiment (ALSE) data over a mare ridge in southeastern Mare Serenitatis show evidence of an anticlinal rise in subsurface horizons and thinning of a mare unit (sequence of flows) on apparent structural relief. The studies of terrestrial analogues supported the compressional tectonic origin involving a combination of folding and thrust faulting (Plescia and Golombek, 1986).

Telescopic studies done from Earth on moon revealed a new kind of troughs called Rillies. They are long, narrow troughs that commonly exhibit three plan view geometries such as sinuous, arcuate and linear. Sinuous rilles are meandrous and confined to mare basalts and interpreted as volcanic in origin and generally thought to be collapsed lava tubes or lava channels (Masursky et al., 1978; Wilhelms, 1987). The relationship between sinuous rillies and mare ridges has been cited as evidence of wrinkle ridges,

which are volcanic in origin (Greeley and Spudis, 1978). Linear and arcuate rilles are found in adjacent to highland and in the margins of mare basins and generally have basins with concentric orientations and flat floored with steep walls (Golombek, 1979; Wilhelms, 1987). The mare ridges and linear rilles have been used to provide constraints on the tectonic evolution of the mare-filled nearside lunar basins (Phillips et al., 1972; Melosh, 1978; Solomon and Head, 1979, 1980: Freed et al., 2001).

Lunar lobate scarps are a class of youngest tectonic landform on the moon that is not directly associated with the mare basins and generally asymmetric landforms and are often lobate segmented. The lobate scarps on Mercury and Mars have over a kilometer of relief, but lunar scarps have a maximum relief of only tens of meters and interpreted as the result of thrust faulting (Howard and Muehlberger, 1973). The wrinkle ridges, arcuate and linear rilles or troughs might be formed due to the lunar localized tectonics. Linear and arcuate rilles express crustal expansion in the basin margins and adjacent highlands whereas wrinkle ridges implies the crustal shortening in the basin interiors. LROC images delineated young lunar lobate scarps globally with tens of meters of relief and interpreted as thrust fault scarps resulting out of global thermal contraction (Watters et al., 2010). Also LROC stereo images provided insights and constraints on the mechanics and kinematics of the formation of tectonic landforms, topography, relief, morphology and regional context on the moon. Contractional tectonic landforms of lobate scarps and wrinkle ridges are discussed as implications of subsurface geometry (Williams et al., 2011). The majority of the previously known lunar scarps are located in the equatorial zone. So far, 14 lobate scarps were detected using NAC images out of that seven occur at latitudes greater than ±60°. The occurrence of previously undetected lobate scarps at high lunar latitudes, along with the distribution of the mid and low latitude scarps on both the near and farside of the moon suggest that, the thrust faults are globally distributed (Watters et al., 2010). Lobate scarps showed the very recent landforms from young tectonic landforms on the moon (Watters and Johnson, 2010), suggesting that they were formed during a recent episode of lunar radial contraction.

There are few outstanding questions to be addressed including the tectonic history of the moon. Determination of global distribution and ages of the lobate scarp thrust faults requires the high-resolution imaging. The next critical question is what is source mechanism for the shallow and deep seated moonquakes? The present mission's data including Kaguya, Chang'E-1, Chandrayaan-1, LRO and GRAIL disclosed detailed information about the critical understanding of the lunar tectonics.

5.5. Lunar space weathering

Space weathering is a process that affects the surfaces of all airless Solar System bodies and it is found that the solar wind is the dominant agent of space weathering. Most of the lunar surface is covered with a layer of fine debris principally produced by impact processes (McKay et al., 1991). Due to unique environment, the lunar soils represent the cumulative product of space weathering. With no atmosphere or magnetic field, cosmic rays and energetic particles of the solar wind constantly wash the surface and space debris of all sizes, bombards the surface at high velocity. In the present scenario, the most frequent interaction of the lunar surface with solid bodies is the smallest micrometeorite particles and multiple cycles of mechanical and irradiation processes alter the physical and compositional properties of lunar soil (Pieters et al., 1993; Heiken et al., 1991). Space weathering occurs at the surface exposed longer time directly to space, has been one of the primary areas of focus of lunar studies for the past several years.

Space weathering causes surfaces to darken, and it causes a relative increase in reflectance with increasing wavelength ("reddening") and changes spectral reflectance signatures of minerals (Pieters et al., 1993). The extensive information on the mechanisms of space weathering could be obtained through comparisons of laboratory spectra of lunar surface samples with remote spectral observations. Lucey et al. (1995) found the suites of lunar soils with restricted ranges of iron contents, but varying maturity form linear trends on a plot of 950 nm/750 nm versus 750 nm reflectance. In the ratio-reflectance plot, the more mature samples plot at the darker, redder end of a trend (Fischer and Pieters, 1994). The space weathering concepts are studied using the high spatial/ spectral resolution lunar surface data for the Swirls region as well as typical spectra of lunar rocks and soils returned from a feldspathic highland (Apollo 16) and a basaltic mare (Apollo 12) site. The lunar swirls help us to understand space weathering processes, that affects the interpretation of remote sensing observations of airless rocky solar system bodies, e.g., Mercury and the asteroids in addition to the moon.

The optical maturity (OMAT) parameter is a measure of the darkening, reddening, and band depth reduction effects of the nanophase iron produced during space weathering. The parameter is defined in such a way that larger values of OMAT correspond to a lesser degree of maturity; that is, higher OMAT = immature (fresher), lower OMAT = more mature. Hence, in the OMAT parameter images, fresh craters appear bright against a darker background of more mature material. A wealth of new data from the Kaguya, Chandrayaan-1, Chang'E-1, and LRO are currently available, and this will lead to further progress in our understanding of the space weathering. Blewett et al. (2011) advocated that, a rover or lander targeted to a prominent albedo and magnetic anomaly and carrying a solar wind spectrometer, Mössbauer spectrometer, X-ray diffraction instrument, UV–visible NIR spectrometer, and a microscopic imager would provide important information on the nature of swirls, the source of magnetic anomalies, and the role of the solar wind in space weathering.

5.6. Lunar quakes

The earthquake study brings more understanding for geoscientists about the structure and interior of the Earth with seismic data (Jin and Zhu, 2003; Jin and Park, 2006; Jin et al., 2007), in analogy, studying moonquake will provide the structure, interior and dynamic activity of the moon. The seismologists can study seismic waves in the subsurface of moon to understand interior and its behavior. With the successful installation of a geophysical station at Hadley brille, on July 31, 1971 on the Apollo 15 mission and the continued operation of stations 12 and 14 approximately 1100 km SW, the Apollo programme for the first time achieved a network of seismic stations on the lunar surface (Latham et al., 1971). Based on the reevaluation of the 1970s Apollo data, "the moon is seismically active" and the possibilities of four different models of moonquakes are suggested (http://science.nasa.gov/science-news/science-at-nasa/2006/15mar_moonquakes). The vibrations from bigger Earthquakes will cease within two minutes, but moonquakes vibration exits more than 10 min like tuning fork. This nature of moonquake is attributed to the presence of water depleted stone, different mineral structure expansion, its dry, cool and rigid surface and interiors. In order to establish longstanding lunar bases, it becomes mandatory to understand the occurrences and nature of moonquakes. This understanding could be achieved by deploying of network seismometers designed to collect precise seismic data's from different regions on moon.

The current understanding of moon is based on existing seismic data, and the more questions arise, which need to be answered by future missions. Compared to Apollo and LROC images, if the wrinkles have grown in the past a few decades, but the moon's diameter has shrunk by just 200 meters in the last billion years, suggesting that recent cooling is relatively small (Watters et al., 2010). In near future, if we wish to set up the base station and think of habitation in the lunar surface, we ought to understand the lunar dynamics, moonquakes and tectonics through geophysical methods such as gravity and seismic study of the moon.

5.7. Future Lunar missions

The past and present lunar missions have provided rock samples and high resolution imaging data to understand the lunar surface features and evolution which developed lot of curiosity among the lunar scientific community. Hence, almost all leading space agencies started planning to send their own mission to the moon. Here, we briefly summarized the upcoming lunar missions' programmes that are already available in the literatures and newsletters. The future lunar missions include the United States GRAIL (end of 2011), China's Chang' E-3 (2013), United States of America's Lunar Atmosphere and Dust Environment Explorer, (LADEE -2013) and International Lunar Network (2018), United Kingdom's Moon Lightweight

Interior and Telecoms Experiment (MoonLITE - 2014), India's Chandrayaan-2, (2014), Russia's Lunar Glob 1 and 2 (2014/2015), which will enable us to resolve the unresolved questions on lunar exploration and sciences.

6. Conclusion

Chang'E-1, SELENE1, Chandrayaan-1 and LRO missions provided a good source of information about the lunar gravity field, surface geomorphology, craters, internal structure and water and the early evolutionary history of the moon. These data were sufficient for basic understanding, but when the question extends to the possibility of human habitability and setting up a permanent base station, more data are required for further understanding of the lunar exploration activities. New missions like Chang'E-2 & 3, SELENE-2, Chandrayaan-2 are expected to provide photo geological, mineralogical and chemical data with which the elemental level chemical mapping can be done. Through that we can understand the stratigraphy and nature of the moon's crust and thereby assessment in certain aspects of magma ocean hypothesis. The higher spatial and spectral images will allow us to determine the compositions of impactors that bombarded the moon during its early evolution which is also relevant to the understanding of Earth formation. These images help us to determine the compositions of the projectiles (asteroid and comets material) from the fresh impact craters, and impact ejecta which are not affected by impact melts, topography, structural features, morphological characters and surface roughness. The major problem in lunar surface is blanketed the original crust by regolith and dust due to impact and space weathering. The central peaks of the older craters and recent impact (fresh) craters allow us to study the compositional information of the original crust of the lunar surface.

Until now, the compositional mapping and topographical studies are almost completed through recent lunar photo geological and imaging spectroscopy data, however, the ground truth information is essential for the strapping conclusion. The samples brought by Apollo missions are extensively utilized as ground truth information to understand the few regions of lunar geology, but further analysis on selected locations will reveal the new results. Hence, this paper suggests that the future missions should aim with rover, pathfinder and sample returned missions for the potential site along with geophysical data, bringing of lunar borehole core sample for the laboratory studies for further understanding of the lunar dynamics, petrogenesis of lunar rocks and evolution to a greater height.

Based on the current knowledge of the geologic setting map of the lunar surface, we have to identify the potential and promising test sites for further exploration with high spatial/ spectral resolution and sample collection. Still the images from the above-mentioned missions are in calibration level, if once the calibrated images are avail-

able to the public domain we could expect much more striking results and new findings from the current and forthcoming lunar mission's data sets, particularly from the near future missions, e.g., GRAIL, Chang' E-3, LADEE, MoonLITE, Chandrayaan-2, SELENE-2, etc.

Acknowledgements

References

Araki, H., Tazawa, S., Noda, H., et al. Lunar global shape and polar topography derived from Kaguya-LALT laser altimetry. Science 323, 897–900, 2009.

Arya, A.S., Rajasekhar, R.P., Thangjam, G., Ajai Kumar, A.S.K. Detection of potential site for future human habitability on the Moon using Chandrayaan-1 data. Curr. Sci. 100, 524–529, 2011.

Atsushi, Y., Sho, S., Sushi, Y.Y., Takayuki, O., Junichi, H., Tatsuaki, O. Lunar tectonics and its implications for the origin and evolution of the moon. Memoirs Geol. Soc. Jpn. 50, 213–226, 1998.

Baldwin, R.B. A Fundamental Survey of the Moon. McGraw-Hill, New York, 1965.

Binder, A.B. Lunar Prospector: overview. Science 281, 1475–1476, 1998.

Blewett, D.T., Coman, E.I., Hawke, B.R., Gillis-Davis, J.J., Purucker, M.E., Hughes, C.G. Lunar swirls: examining crustal magnetic anomalies and space weathering trends. J. Geophys. Res. 116, E02002, http://dx.doi.org/10.1029/2010JE003656, 2011.

Bokun, Y., Runsheng, W., Fuping, G., Zhenchao, W. Minerals mapping of the lunar surface with Clementine UVVIS/NIR data based on spectra unmixing method and Hapke model. Icarus 208, 11–19, 2010.

Cahill, J.T.S., Lucey, P.G., Wieczorek, M.A. Compositional variations of the lunar crust: results from radiative transfer modelling of central peak spectra. J. Geophys. Res. E114, E09001, 2009.

Chambers, J.G., Taylor, L.A., Patchen, A. Quantitative mineralogical characterization of lunar high-Ti mare basalts and soils for oxygen production. J. Geophys. Res. 100 (E7), 14 391–14 401, 1995.

Chin, G., Brylow, S., Foote, M., et al. Lunar reconnaissance orbiter overview: the instrument suite and mission. Space Sci. Rev. 129, 391–419, http://dx.doi.org/10.1007/s11214-007-9153, 2007.

Colaprete, A., Schultz, P., Heldmann, J., et al. Detection of water in the LCROSS ejecta plume. Science 330 (6003), 463–468, http://dx.doi.org/10.1126/science.1186986, 2010.

Crawford, I.A., Joy, K.H., Kellett, B.J., et al. The scientific rationale for the C1XS X-ray spectrometer on India's Chandrayaan-1 mission to the moon. Planet Space Sci. 57 (7), 725–734, 2009.

Crider, D.H., Vondrak, R.R. Hydrogen migration to the lunar poles by solar wind bombardment of the moon. Adv. Space Res. 30 (8), 1869–1874, 2002.

Dunkin, S.K., Heather, D.J. Remote sensing of the moon: the past, present and future, in: ICEUM4, 10–15th July 2000, ESTEC, Noordwijk, The Netherlands, 2000.

Fa, W.Z., Jin, Y.Q. Global inventory of Helium-3 in lunar regoliths estimated by a multi-channel microwave radiometer on the Chang-E 1 lunar satellite. Chin. Sci. Bull. 55, 4005–4009, 2010.

Feldman, W.C., Maurice, S., Binder, A.B., Barraclough, B.L., Elphic, R.C., Lawrence, D.J. Fluxes of fast and epithermal neutrons from lunar prospector: evidence for water ice at the lunar poles. Science 281, 1496, http://dx.doi.org/10.1126/science.281.5382.1496, 1998.

Feldman, W.C., Lawrence, D.J., Elphic, R.C., Barraclough, B.L., Maurice, S., Genetay, L., Binder, A.B. Polar hydrogen deposits on the moon. J. Geophys. Res. 105 (E2), 4175–4196, 2000.

Feldman, W.C., Maurice, S., Lawrence, D.J., Little, R.C., Lawson, S.L., Gasnault, O., Wiens, R.C., Barraclough, B.L., Elphic, R.C., Prettyman, T.H., Steinberg, J.T., Binder, A.B. Evidence for water ice near the lunar poles. J. Geophys. Res. 106, 23231–23252, 2001.

Fischer, E.M., Pieters, C.M. Remote determination of exposure degree and iron concentration of lunar soils using VIS-NIR spectroscopic methods. Icarus 111, 475–488, 1994.

Freed, A.M., Melosh, H.J., Solomon, S.C. Tectonics of mascon loading; Resolution of the strike-slip faulting paradox. J. Geophys. Res. 106, 20603–20620, 2001.

Gilbert, G.K. The Moon's face, a study of the origin of its features, Philos. Soc. Washington Bull., 12, pp. 241–292, 1893.

Gladstone, G.R., Hurleu, D.M., Retherford, K.D., et al. LRO-LAMP observations of the LCROSS impact plume. Science 330 (6003), 472–476, http://dx.doi.org/10.1126/science.1186474, 2010.

Glotch, T.D., Lucey, P.G., Bandfield, J.L., Greenhagen, B.T., Thomas, I.R., Elphic, R.C., Bowles, N., Wyatt, M.B., Allen, C.C., Hanna, K.D., Paige, D.A. Highly silicic compositions on the moon. Science 329 (5998), 1510–1513, 2010.

Golombek, M.P. Structural analysis of lunar grabens and the shallow crustal structure of the moon. J. Geophys. Res. 88, 3563–3578, 1979.

Goswami, J.N., Annadurai, M. Chandrayaan-1: India's first planetary science mission to the moon. Current Sci. 96, 486–491, 2009.

Graham, D.G., Muenow, D.W., Gibson Jr., E.K., Some effects of gas adsorption on the high temperature volatile release behavior of a terrestrial basalt, tektite and lunar soil, in: Proceedings of the 10th Lunar and Planetary Science Conference, Houston, TX, USA, 2, pp. 1617–1627, 1979.

Grande, M., Maddison, B.J., Howe, C.J., et al. The C1XS X-ray spectrometer on Chandrayaan-1. Planet. Space Sci. 57, 717–724, http://dx.doi.org/10.1016/j.pss.2009.01.016, 2009.

Greeley, R., Spudis, P.D., Mare volcanism in the Herigonius region of the moon, in: Proc. Lunar Planet. Sci. Conf. 9, pp. 3333–3349, 1978.

Greenhagen, B.T., Lucey, P.G., Wyatt, M.B., Glotch, T.D., Allen, C.C., Arnold, J.A., Bandfield, J.L., Bowles, N.E., Hanna, K.L.D., Hayne, P.O., Song, E., Thomas, I.R., Paige, D.A. Global silicate mineralogy of the moon from the diviner lunar radiometer. Science 329, 1507–1509, 2010.

Han, S.C. Improved regional gravity fields on the Moon from Lunar Prospector tracking data by means of localized spherical harmonic functions. J. Geophys. Res. 113, E11012, http://dx.doi.org/10.1029/2008JE003166, 2008.

Han, S.C., Mazarico, E., Lemoine, F.G. Improved nearside gravity field of the Moon by localizing the power law constraint. Geophys Res Lett 36, L11203, 2009.

Hansen, T.P. Guide to Lunar Orbiter Photographs: lunar orbiter photographs and maps missions 1 through 5. NASA SP-242, 254, N71-36179, 1970.

Hapke, B. Space weathering from Mercury to the asteroid belt. J. Geophys. Res. E106, 10039–10073, 2001.

Hartmann, W.K., Wood, C.A. Moon: origin and evolution of multi ring basins. The Moon 3, 3–78, 1971.

Haruyama, J., Ohtake, M., Matsunaga, T., et al. Long-lived volcanism on the lunar Farside revealed by SELENE Terrain Camera. Science 323 (5916), 905–908, 2009.

S. Jin et al. / Advances in Space Research 52 (2013) 285–305

Haruyama, J., Ohtake, M., Matsunaga, T., et al. Lack of exposed ice inside lunar south pole Shackleton crater. Science 322 (5903), 938–939, 2008.

Hawke, B.R., Peterson, C.A., Blewett, D.T., Bussey, D.B.J., Lucey, P.G., Taylor, G.J., Spudis, P.D. Distribution and modes of occurrence of lunar anorthosite, J. Geophys. Res. 108 (E6), 5050, http://dx.doi.org/10.1029/2002JE001890, 2003.

Head, J.W., Wilson, L. Absence of large shield volcanoes and calderas on the moon: consequence of Magma transport phenomena? Geophys. Res. Lett. 18 (11), 2121–2124, 1991.

Head, J.W., Gifford, A. Lunar mare domes: classification and mode of origin. The Moon and Planets 22, 235–258, 1980.

Heiken, G.H., Vaniman, D.T., French, B.M. Lunar Sourcebook: A User's Guide to the Moon, Cambridge University Press, Cambridge, 1991.

Howard, K.A., Muehlberger, W.R. Lunar thrust faults in the Taurus-Littrow region, Apollo 17 Prel. Sci. Rep., NASA Spec. Publications, SP-330, pp. 31-23–31-25, 1973.

Isaacson, P.J., Pieters, C.M., Besse, S., Clark, R.N., Head, J.W., Klima, R.L., Mustard, J.F., Petro, N.E., Staid, M.I., Sunshine, J.M., Taylor, L.A., Thaisen, K.G., Tompkins, S. Remote compositional analysis of lunar olivine-rich lithologies with Moon Mineralogy Mapper (M3) spectra. J. Geophys. Res. 116 (E00G11), http://dx.doi.org/10.1029/2010JE003731, 2011.

Ishihara, Y., Goossens, S., Matsumoto, K., Noda, H., Araki, H., Namiki, N., Hanada, H., Iwata, T., Tazawa, S., Sasaki, S. Crustal thickness of the moon: implications for farside basin structures. Geophys. Res. Lett. 36, L19202, http://dx.doi.org/10.1029/2009GL039708, 2009.

Ishihara, Y., Morota, T., Nakamura, R., Goossens, S., Sasaki, S. Anomalous Moscoviense basin: single oblique impact or double impact origin? Geophys. Res. Lett. 38, L03201, http://dx.doi.org/10.1029/2010GL045887, 2011.

Jin, S.G., Zhu, W.Y. Active motion of tectonic blocks in Eastern Asia: evidence from GPS measurements. ACTA Geol. Sin. 77 (1), 59–63, 2003.

Jin, S.G., Park, P.H. Strain accumulation in South Korea inferred from GPS measurements. Earth Planet. Space 58 (5), 529–534, 2006.

Jin, S.G., Park, P., Zhu, W. Micro-plate tectonics and kinematics in Northeast Asia inferred from a dense set of GPS observations. Earth Planet. Sci. Lett. 257 (3–4), 486–496, http://dx.doi.org/10.1016/j.epsl.2007.03.011, 2007.

Jin, S.G. Preface: recent results on lunar exploration and science. Adv. Space Res. 50 (12), 1581–1582, http://dx.doi.org/10.1016/j.asr.2012.09.010, 2012.

Kumar, A.S.K., Chowdhury, A.R., Banerjee, A., Dave, A.B., Sharma, B.N., Shah, K.J., Murali, K.R., Joshi, S.R., Sarkar, S.S., Patel, V.D. Terrain mapping camera: a stereoscopic high-resolution instrument on Chandrayaan-1. Curr. Sci. 96, 492–495, 2009.

Lafrance, B., John, B.E., Scoates, J.S. Syn-emplacement recrystallization and deformation microstructures in the Poe Mountain anorthosite. Wyoming. Contrib. Mineral. Petrol. 122, 431–440, 1996.

Latham, G., Ewing, M., Dorman, J., Lammlein, D., Press, F., Toksoz, N., Sutton, G., Duennebier, F., Nakamura, Y. Moonquakes and lunar tectonism. The Moon 4 (3–4), 373–382, 1971.

Lawrence, D.J., Feldman, W.C., Elphic, R.C., Hagerty, J.J., Maurice, S., McKinney, G.W., Prettyman, T.H. Improved modeling of Lunar Prospector neutron spectrometer data: implications for hydrogen deposits at the lunar poles. J. Geophys. Res. 111, E08001, http://dx.doi.org/10.1029/2005JE002637, 2006.

Li, C., Ren, X., Liu, J., et al. Laser altimetry data of Chang'E-1 and the global lunar DEM model. Sci. China- Earth Sci. 53 (1), 1582–1593, 2010.

Ling, Z., Zhang, J., Liu, J., et al. Preliminary results of FeO mapping using imaging interferometer data from Chang'E-1. Chin. Sci. Bull. 56 (4–5), 376–379, 2011.

Liu, F., Shi, J., Le, Q., Rong, Y. Lunar Titanium characterization based on Chang'E (CE-1) interference imaging spectrometer (IIM) imagery and RELAB spectra, in: 41st Lunar and Planetary Science Conference, Abstract # 1642, 2010.

Lucey, P.G., Taylor, G., Malaret, E. Abundance and distribution of Iron on the moon. Science 268, 1150–1153, 1995.

Lucey, P.G. Mineral maps of the moon. Geophys. Res. Lett. 31, L08701, 2004.

Lucey, P.G., Blewett, D.T., Jolliff, B.L. Lunar iron and titanium abundance algorithms based on final processing of Clementine ultraviolet-visible images. J. Geophys. Res. 105 (E8), 20 297–20 305, 2000.

Lucey, P.G. A lunar waterworld. Science 326 (5952), 531–532, http://dx.doi.org/10.1126/science.1181471, 2009.

Mao, H.K., Bell, P.M. Crystal-field effects in spinel: oxidation states of iron and chromium. Geochim. Cosmochim. Acta 39 (6–7), 865–866, 1975.

Masursky, H., Colton, G.W., El-Baz, F. Apollo Over the Moon: A View from Orbit. NASA Spec. Publ., SP-362, 1978.

Matsumoto, K., Goossens, S., Ishihara, Y., et al. An improved lunar gravity field model from SELENE and historical tracking data: revealing the farside gravity features. J. Geophys. Res. 115, E06007, http://dx.doi.org/10.1029/2009JE003499, 2010.

McCallum, I.S. A new views of the moon in light of data from Clementine and Prospector missions. Earth Moon Planet. 85–86, 253–269, 2001.

McEwen, A.S., Robinson, M.S. Mapping of the moon by Clementine. Adv. Space Res. 19, 1523–1533, 1997.

McKay, D.S., Heiken, G., Basu, A., Blanford, G., Simon, S., Reedy, R., French, B.M. The lunar regolith, in: Heiken, G.H., Vaniman, D.T., French, B.M. (Eds.), Lunar Source Book. Cambridge Univ. Press, New York, pp. 285–356, 1991.

Melosh, H.J. The tectonics of mascon loading. Proc. Lunar Planet. Sci. Conf. 9, 3513–3525, 1978.

Meng, Z.G., Chen, S.B., Edward, M.O., et al. Research on water ice content in Cabeus crater using the data from the microwave radiometer onboard Chang'E-1 satellite. Sci. China Phys. Mech. Astron. 53, 2172–2178, 2010.

Mitrofanov, I.G., Sanin, A.B., Boynton, W.V., et al. Hydrogen mapping of the lunar South pole using the LRO neutron detector experiment LEND. Science 330 (6003), 483–486, 2010.

Murcray, F.H., Murcray, D.G., Williams, W.J. Infrared emissivity of lunar surface features 1 Balloon-Borne observations. J. Geophys. Res. 75 (14), 2662–2669, 1970.

Nakamura, R., Matsunaga, T., Ogawa, Y., et al. Ultramafic impact melt sheet beneath the South Pole-Aitken basin on the moon. Geophys. Res. Lett. 36, L22202, 2009.

Namiki, N., Iwata, T., Matsumoto, K., et al. Farside gravity field of the moon from four-way doppler measurements of SELENE (Kaguya). Science 323 (5916), 900–905, 2009.

Nozette, S., Rustan, P., Pleasance, L.P., et al. The Clementine mission to the moon: scientific overview. Science 266 (5192), 1835–1839, 1994.

Ogawa, K., Okada, T., Shira, K., Kato, M. Numerical estimation of lunar X-ray emission for X-ray spectrometer onboard SELENE. J. Earth Planet. Space 60 (4), 283–292, 2008.

Ohtake, M., Haruyama, J., Matsunaga, T., Yokota, Y., Morota, T., Honda, C., LISM team Performance and scientific objectives of the SELENE (KAGUYA) Multiband Imager. Earth Planet. Space 60, 257–264, 2008.

Ohtake, M., Matsunaga, T., Haruyama, J. The global distribution of pure anorthosite on the moon. Nature 461, 236–240, http://dx.doi.org/10.1038/nature08317, 2009.

Ono, T., Kumamoto, A., Nakagawa, H., Yamaguchi, Y., Oshigami, S., Yamaji, A., Kobayashi, T., Kasahara, Y., Oya, H. Lunar Radar Sounder observations of subsurface layers under the nearside maria of the moon. Science 323 (5916), 909–912, 2009.

Ouyang, Z., Li, C., Zhou, Y., et al. Chang'E-1 lunar mission: an overview and primary science results. Chin. J. Space Sci. 30 (5), 392–403, 2010.

Papike, J.J., Hodges, F.N., Bence, A.E., Cameron, M., Rhodes, J.M. Mare basalts: crystal chemistry, mineralogy, and petrology. Rev. Geophys. 14 (4), 475–540, 1976.

Paige, D.A., Siegler, M.A., Zhang, J., et al. Diviner lunar radiometer observations of cold traps in the moon's South polar region. Science 330 (6003), 479–482, 2010.

Phillips, R.J., Conel, J.E., Abbott, E.A., Sjogren, W.L., Morton, J.B. Mascons: progress toward a unique solution for mass distribution. J. Geophys. Res. 77, 7106–7114, 1972.

Pieters, C.M., Goswami, J.N., Clark, R.N., et al. Character and Spatial Distribution of OH/H$_2$O on the surface of the moon seen by M3 on Chandrayaan-1. Science 326 (5952), 568–572, 2009.

Pieters, C.M., Besse, S., Boardman, J., et al. Mg- spinel lithology: a new rock-type on the lunar farside, J. Geophys. Res., 2010JE003727, 2011.

Pieters, C., Fischer, E.M., Rode, O., Basu, A. Optical effects of space weathering: the role of the finest fraction. J. Geophys. Res. 98, 20 817–20 824, 1993.

Pinet, P.C., Chevrel, S.D., Martin, P. Copernicus: a regional probe of the lunar interior. Science 260, 797–801, 1993.

Plescia, J.B., Golombek, M.P. Origin of Planetary wrinkle ridges based on the study of terrestrial analogs. Geol. Soc. Am. Bull. 97, 1289–1299, 1986.

Quaide, W.L. Rilles, ridges and domes-Clues to maria history. Icarus 4 (4), 374–389, 1965.

Robinson, M.S., Eliason, E.M., Hiesinger, H., Jolliff, B.L., McEwen, A.S., Malin, M.C., Ravine, M.A., Thomas, P.C., Turtle, E.P., Cisneros, E.B., The LROC Team. Lunar reconnaissance orbiter camera: first results, in: 41st Lunar and Planetary Science Conference, Abstract # 1874, 2010.

Robinson, M., Riner, M. Advances in lunar science from the Clementine mission: a decadal perspective. J. Earth Syst. Sci. 114 (6), 669–686, 2005.

Saal, A.E., Hauri, E.H., Cascio, M.L., van Orman, J.A., Rutherford, M.C., Cooper, R.F. Volatile content of lunar volcanic glasses and the presence of water in the moon's interior. Nature 454, 192–195, http://dx.doi.org/10.1038/nature07047, 2008.

Salisbury, J.W., Walter, L.S. Thermal infrared (2.5–13.5) spectroscopic remote sensing of igneous rock types on particulate planetary surfaces. J. Geophys. Res. 94 (B7), 9192–9202, 1989.

Schultz, P.H., Staid, M., Pieters, C.M. Recent lunar activity: evidence and implications, in: 31st Lunar and Planetary Science Conference, Abstract # 1919, 2000.

Schultz, P.H., Staid, M.I., Pieters, C.M. Lunar activity from recent gas release. Nature 444, 184–186, http://dx.doi.org/10.1038/nature05303, 2006.

Smith, D.E., Zuber, M.T., Jackson, G.B., et al. The lunar orbiter laser altimeter investigation on the lunar reconnaissance orbiter mission. Space Sci. Rev. 150, 209–241, 2010a.

Smith, D.E., Zuber, M.T., Neumann, G.A., et al. Initial observations from the Lunar Orbiter Laser Altimeter (LOLA). Geophy. Res. Lett. 37, L18204, http://dx.doi.org/10.1029/2010GL043751, 2010b.

Solomon, S.C., Head, J.W. Vertical movement in mare basins: relation to mare emplacement, basin tectonics and lunar thermal history. J. Geophys. Res. 84, 1667–1682, 1979.

Solomon, S.C., Head, J.W. Lunar mascon basins: lava filling, tectonics, and evolution of the lithosphere. Rev. Geophys. Space Phys. 18, 107–141, 1980.

Spudis, P.D., Volcanism on the moon, in: Encyclopedia of Volcanoes, Academic Press, pp. 697–708, 2000.

Spudis, P.D., Hawke, B.R., Lucey, P. Composition of Orientale basin deposits and implications for the lunar basin-forming process, in: Proc. 15th Lunar and Planetary Science Conference, pp. C197–C210, 1984.

Spudis, P.D., Bussey, D.B.J., Baloga, S.M., et al. Initial results for the North pole of the moon from Mini-SAR, Chandrayaan-1 mission. Geophys. Res. Lett. 37, L06204, http://dx.doi.org/10.1029/2009GL042259, 2010.

Staid, M., Isaacson, P., Petro, N., Boardman, J., Pieters, C.M., Head, J.W., Sunshine, J., Hanna, K.D., Taylor, L.A., The M3 Team. The spectral properties of INA: new observations from the moon mineralogy mapper, in: 42nd Lunar and Planetary Science Conference, Abstract # 2499, 2011.

Staid, M.I., Pieters, C.M. Integrated spectral analysis of mare soils and craters: applications to eastern nearside basalts. Icarus 145, 122–139, http://dx.doi.org/10.1006/icar.1999.6319, 2000.

Starukhina, L.V., Shkuratov, Y.G. The lunar poles: water ice of chemically trapped hydrogen? Icarus 147, 585–587, 2000.

Stephen, L., Gillett. Economic geology of the moon: some concentrations, in: Lunar and Planetary Institute Technical Report, NASA Astrophysics Data System, 92-06, pp. 29–30, 1992.

Stoffler, D., Knoll, H.-D., Marvin, U.B., Simonds, C.H., Warren, P.H. Recommended classification and nomenclature of lunar highland rocks-A committee report, in: Papike, J.J., Merrill, R.B. (Eds.), Proceedings of the Conference on Lunar Highlands Crust, Pergamon, NY, pp. 51–70.

Su, X., Huang, Q., Yan, J., Ping, J. The improved topographic model from Chang'E-1 mission, in: 42nd Lunar and Planetary Science Conference, Abstract # 1077, 2011.

Sugano, T., Heki, K. Isostasy of the Moon from high-resolution gravity and topography data: Implication for its thermal history. Geophys. Res. Lett. 31, L24703, http://dx.doi.org/10.1029/GL022059, 2004.

Thomson, B.J., Bussey, D.B.J., Cahill, J.T.S., Neish, C., Patterson, G.W., Spudis, P.D. The Interior of Shackleton crater as revealed by Mini-RF orbital radar, in: 42nd Lunar and Planetary Science Conference, Abstract # 1626, 2011.

Tjia, H.D. Lunar wrinkle ridges indicative of strike-slip faulting. Geol. Soc. Am. Bull. 81, 3095–3100, 1970.

Tompkins, S., Pieters, C.M. Mineralogy of the lunar crust: results from Clementine. Meteorit. Planet. Sci. 34, 25–41, 1999.

Wang, X.-D., Zong, Q.-G., Wang, J.-S., et al. Detection of $m/q = 2$ pickup ions in the plasma environment of the moon: the trace of exospheric H$_2^+$. Geophys. Res. Lett. 38, L14204, http://dx.doi.org/10.1029/2011GL047488, 2011.

Warren P.H., Bridges J.C. Lunar meteorite Yamato-983885: A relatively KREEPy regolith breccia not paired with Y-791197, in: 67th Annual Meteoritical Society Meeting, August 2–6, 2004, Rio de Janeiro, Brazil, Abstract No. 5095, 2004.

Watson, K., Murray, B.C., Brown, H. The behavior of volatiles on the lunar surface. J. Geophys. Res. 66 (9), 3033–3045, http://dx.doi.org/10.1029/JZ066i009p03033, 1961.

Watters, T.R., Schultz, R.A. Planetary tectonics: introduction, in: Watters, T.R., Schultz, R.A. (Eds.), Planetary Tectonics, Cambridge University Press, pp. 1–14, 2010.

Watters, T.R., Johnson, C.L. Lunar tectonics, in: Watters, T.R., Schultz, R.A. (Eds.), Planetary Tectonics, Cambridge University Press, pp. 121–182, 2010.

Watters, T.R., Robinson, M.S., Beyer, R.A., Banks, M.E., Bell, J.F., Pritchard, M.E., Hiesinger, H., Bogert, C.H.V., Thomas, P.C., Turtle, E.P., Williams, N.R. Evidence of recent thrust faulting on the moon revealed by the lunar reconnaissance orbiter camera. Science 329, 936–940, 2010.

Watts, A.B. Isostasy and Flexure of the Lithosphere, Cambridge Univ. Press, NY, 2001.

Wieczorek, M.A., Jolliff, B.L., Khan, A., et al. The constitution and structure of the lunar interior. Rev. Mineral. Geochem. 60, 221–364, 2006.

Wilcox, B.B., Lucey, P.G., Gillis, J.J. Mapping iron in the lunar mare: an improved approach. J. Geophys. Res. 110, E11001, http://dx.doi.org/10.1029/2005JE002512, 2005.

Wilhelms, D.E. The Geologic History of the Moon. US Government Printing Office, Washington, DC, 1987.

Williams, N.R., Pritchard, M.E., Bell, J.F., et al. Two tectonic landforms from lunar reconnaissance orbiter camera digital terrain models, in: 42nd Lunar and Planetary Science Conference, Abstract # 1624, 2011.

Yamamoto, S., Nakamura, R., Matsunaga, T., et al. Possible mantle origin of olivine around lunar impact basins detected by SELENE. Nat. Geosci. 3, 533–536, http://dx.doi.org/10.1038/ngeo897, 2010.

Zheng, Y.C., Wang, S.J., Ouyang, Z.Y. Dielectric properties of lunar material and its microwave penetration depth. J. Geochim. Cosmochim. Acta 69 (10), A805, 2005.

Zheng, Y., Ouyang, Z., Li, C., Liu, J., Zou, Y. China's lunar exploration program: present and future. Planet. Space. Sci. 56, 881–886, 2008.